Norwegian Meteorological Institute

METreport

No. 4/2021
ISSN 2387-4201
Climate

Homogenization of Norwegian monthly precipitation series for the period 1961-2018

Elinah Khasandi Kuya, Herdis Motrøen Gjelten, Ole Einar Tveito

Norwegian Meteorological Institute

METreport

Title
Homogenization of Norwegian monthly precipitation series for the period 1961-2018

Date
2021-04-30

Section
Division for Climate Services

Report no.
No. 4/2021

Author(s)
Elinah Khasandi Kuya, Herdis Motrøen Gjelten, Ole Einar Tveito

Classification
● Free ○ Restricted

Abstract
Climatol homogenization method was applied to detect inhomogeneities in Norwegian precipitation series, during the period 1961-2018. 370 series (including 44 from Sweden and one from Finland) of monthly precipitation sums, from the ClimNorm precipitation dataset were used in the analysis. The homogeneity analysis produced a 58-year long homogenous dataset for 325 monthly precipitation sum with regional temporal variability and spatial coherence that is better than that of non-homogenized series. The dataset is more reliable in explaining the large-scale climate variations and was used to calculate the new climate normals in Norway.

Keywords
Homogenization, climate normals, precipitation

Disciplinary signature

Responsible signature

Abstract

Climate normals play an important role in weather and climate studies and therefore require high-quality dataset that is both consistent and homogenous. The Norwegian observation network has changed considerably during the last 20-30 years, introducing non-climatic changes such as automation and relocation. Homogenization was therefore necessary and work has been done to establish a homogeneous precipitation reference dataset for the purpose of calculating the new climatological standard normals for the period 1991-2020. The homogenization tool Climatol was applied to detect inhomogeneities in the Norwegian precipitation series for the period 1961-2018. 370 series (including 44 from Sweden and one from Finland) of monthly precipitation sums, from the ClimNorm precipitation dataset were used in the analysis. The primary goal of this analysis was to establish a high-quality precipitation reference dataset, which is both consistent and homogeneous, for calculation of the new standard climate normals (1991-2020). Results from homogeneity testing found inhomogeneities in 95 (29 %) of the 325 Norwegian precipitation series, however, only 81 (25 %) were classified as inhomogeneous after conferring with metadata and therefore adjusted. Relocation of the precipitation gauge and automation were the main causes of all the inhomogeneities in the Norwegian series, explaining 71 % and 12 % respectively of all detected breaks. All but one of the accepted inhomogeneities could be confirmed with metadata. Results further showed benefits of incorporating metadata to the automatically detected inhomogeneities. Linear trend analysis showed increasing trends in the period 1961-2018 except in autumn where a decreasing trend was observed. The homogeneity analysis produced a 58-year long homogenous dataset for 325 monthly precipitation series with better regional temporal variability and spatial coherence than that of the non-homogenized series. The dataset is more reliable in explaining the large-scale climate variations and was used to calculate the new climate normals in Norway.

Meteorologisk institutt
Meteorological Institute
Org.no 971274042
post@met.no

Oslo
P.O. Box 43 Blindern
0313 Oslo, Norway
T. +47 22 96 30 00

Bergen
Allégaten 70
5007 Bergen, Norway
T. +47 55 23 66 00

Tromsø
P.O. Box 6314, Langnes
9293 Tromsø, Norway
T. +47 77 62 13 00

www.met.no

Table of contents

1 Introduction

A common practice in datasets that are to be used in the monitoring and analysis of long time climate change and variability studies is to establish the homogeneity of the underlying time series. Homogenization of Norway's monthly precipitation series was therefore undertaken to establish a high quality precipitation reference dataset for calculating new standard climate normal for the period 1991-2020. Climate normals play an important role in weather and climate studies and therefore require high quality data that are both consistent and homogenous. Long-term climatological time series is regarded as homogeneous if the measurements have been consistently done using the same practices, with the same undamaged instruments at the same place and time and in the same environment. This way the variations in the time series are only as a result of variations in weather and climate. But the reality is that many climatic observations have been altered by a variety of external changes such as changes in instruments, observers, observation methods and practices, the station's geographical location and in the environment surrounding the station. Such changes can introduce sudden shifts (homogeneity breaks) to the time series; others, e.g. environmental changes, lead to gradual biases over time. This can mask the genuine climatic variations and can lead to erroneous interpretations about the evolution of climate (Peterson et al., 1998). Since these shifts and biases are often of the similar magnitude as the climate signal (Menne et al., 2009), analyzing and correcting for such external influences to achieve a homogeneous climatic time series is therefore necessary before making a climate assessment.

Several applications have been developed to detect inhomogeneities in climate series (WMO, 2020) including the new emerging techniques HOMER (Mestre et al., 2013), ACMANT (Domonkos, 2015; Domonkos and Coll, 2017a), AHOPS (Rustemeier et al., 2017) and Climatol (Guijarro, 2018). The homogeneity approaches often benefit from consulting metadata to validate the breaks and possible outliers.

Homogenization of long-term precipitation series for mainland Norway has previously been done by Hanssen-Bauer and Førland (1994) using the Standard Normal Homogeneity Test (SNHT) (Alexandersson, 1986). The study analyzed 165 Norwegian precipitation series whereby 70 % of the series were found to be inhomogeneous. Long-term series from the Norwegian Arctic were later homogenized by Nordli et al. (1996) using SNHT. Several inhomogeneities were detected in the Arctic precipitation series, and were linked to errors in the undercatch of the precipitation gauges especially for snow, which under windy conditions is sensitive to minor changes in the environment. The most recent homogenization analysis in MET on precipitation was done within the MIST-2 project, a collaboration between MET and Statkraft SF (Lundstad, 2016) to homogenize daily precipitation series in Norway. Five precipitation series representing different energy consumption regions in Norway were successfully homogenized applying three different homogenization softwares with different time resolution; HOMER (Mestre et al., 2013), MASH (Szentimrey, 1999, 2014) and RHtest (Wang & Feng, 2013, 2014).

Comprehensive analysis on long precipitation series, covering the entire mainland Norway (Hanssen-Bauer and Førland, 1994) was done more than 20 years ago. The precipitation observation network has since undergone several changes including geographical relocation of stations, change in precipitation measurement technology and observation routines. The most significant change has been the automation of stations together with the reduction of the number of stations in the precipitation network since the late 80s.

This study is part of the “Klimanormaler 1991-2020” project at MET Norway, and also the ClimNorm project, an international network activity under the Nordic Framework for Climate Services (NFCS) (Tveito et al., 2020), covering 6 countries in the Nordic region (Denmark, Estonia, Finland, Latvia, Norway and Sweden). This report will establish a homogeneous precipitation reference dataset for 325 monthly precipitation series for mainland Norway for the period 1961-2018, using Climatol (Guijarro, 2018). This is a continuation of a similar report on homogenization of monthly mean temperature time series for Norway (Kuya et al., 2020).

2 Data and methods

2.1 Precipitation dataset

Precipitation time series used in this study were extracted from the ClimNorm precipitation dataset (Tveito et al., 2020). ClimNorm is a collaboration between climate services in Denmark, Estonia, Finland, Latvia, Norway and Sweden with an objective that includes sharing data, methods and experiences in preparing a data basis as good as possible for calculation of new climate normals.

548 series (including 50 from Sweden and 2 from Finland) were available from the ClimNorm dataset for the homogenization of Norway's precipitation series. All of the series covered the period 1961-2018, but many of the series had gaps. 370 series upheld the criteria of 80 % data coverage (no more than ten missing years) in the period 1961-2018 and were therefore used in the analysis. 33 % of the 370 series were merged and these were reconstructed from up to four original series. The criteria for merging time series was based on a maximum horizontal distance of 10 km, and after the first automatic screening all merged series were manually checked (Tveito et al., 2020).

370 series of monthly precipitation sums were used in the homogenization analysis see Fig. 1. This included 325 series from mainland Norway, 44 Swedish series and one Finnish series. The analyzed time-period was 1961-2018. Because the goal was to have a homogeneous data set for the period of new normals, i.e. 1991-2020, the analyzed period was extended back to 1961 since longer time series gives a more robust result when homogenizing.

2.2 Climatol

Climatol (Guijarro, 2018, 2019) was used for the homogenization of Norway’s monthly precipitation series. Climatol is a relative homogenization method that was developed under the R program (R Core Team, 2015). It is based on the Standard Normal

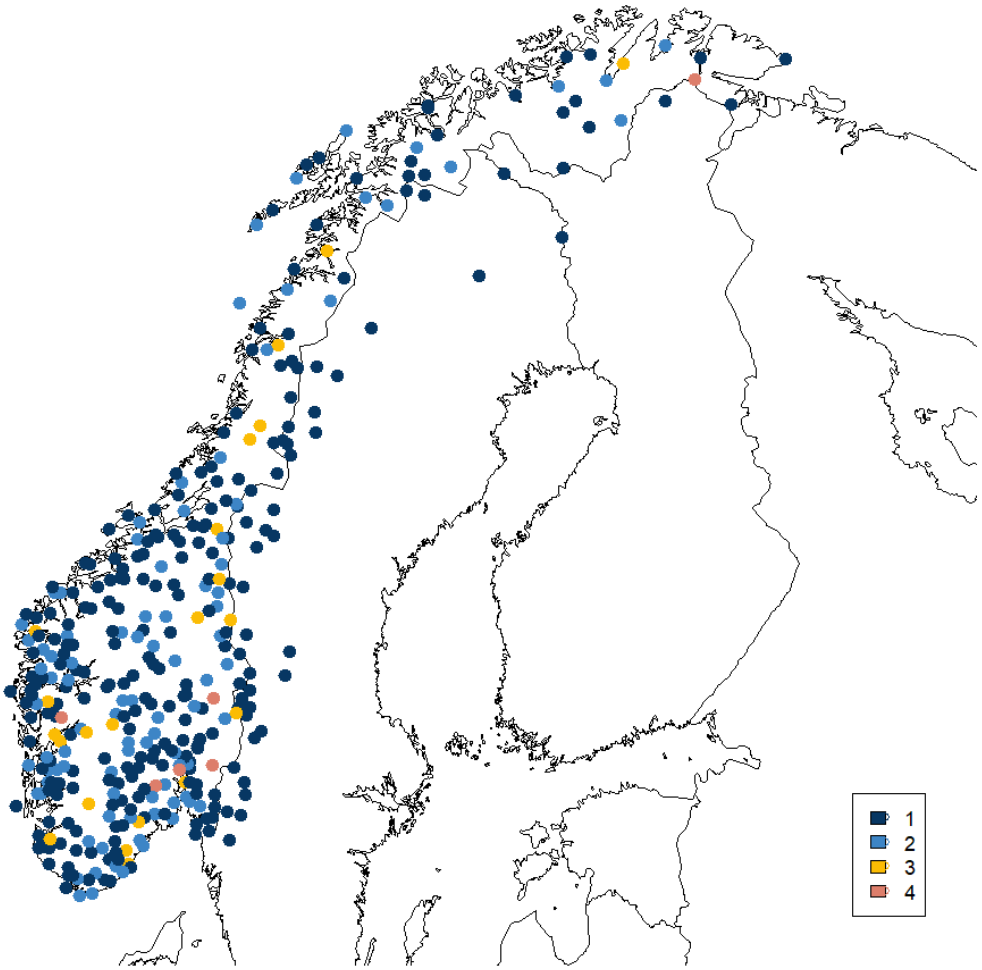

Figure 1: Location of stations used in the study. The colours denote if the series is merged and if so, how many series are included in the merged series.

Homogeneity Test (SNHT) by Alexandersson (1986), which was later modified by Alexandersson and Moberg (1997).

Climatol has been widely used to homogenize a variety of climate variables including temperature, precipitation and wind (Guijarro, 2008, 2015; Luna et al., 2012; Mamara et al., 2013; Azorin-Molina et al., 2016, 2018, 2019; Ponce-Cruz et al., 2019; and Coll et al., 2020). In their analysis, Coll et al. (2020) concluded that Climatol's break frequency results seemed closest to reality among the four homogenization methods they examined including HOMER, ACMANT and AHOPS. Version 3.1.1 of the Climatol package that provides automatic quality control (outlier correction), homogenization (break detection and correction) and missing data attribution was therefore used in this analysis. This method is excellent for the detection and adjustment of inhomogeneities of large and dense networks and has the option to incorporate metadata information.

In the detection and adjustment phase, the homogeneity methods can be categorized as either absolute or relative. Relative homogenization methods are more robust than absolute methods because they rely on comparison of correlated neighboring stations, which are often exposed to the same climate signal. The absolute method is applied directly to individual series to identify statistically significant breakpoints. The absolute method does not use any neighboring series in the analysis and this results in much larger uncertainties of the homogenized series. Noise in the series, partially from long-term variations in the climate system, makes it harder to distinguish inhomogeneities from uncorrelated noise when no neighboring series are used as reference. In their blind intercomparison and validation study for monthly homogenization algorithms, Venema et al. (2012) concluded that applying the state of the art relative homogenization algorithms developed to work with an inhomogeneous reference gives better results.

Relative homogenization methods assume that the precipitation amounts in a candidate series[1] are proportional to some regional averages as shown by Paulhus and Kohler (1952). Climatol is highly dependent on difference series between a candidate series and its reference series. The difference series is estimated as a weighted average of the nearest and best correlated reference series. Correlation between the series is fundamental, because the higher the correlation, the higher the reliability of the homogenization and in filling of missing data. Correlations are generally a function of the distance, and therefore reduce when distance between stations is greater. However, sharp geographic discontinuities (e.g. high mountains) can produce opposite regimes and as such nearby stations can be badly correlated.

The description of Climatol in the following sections is gathered from Guijarro (2018) and the Climatol user manual which can be found on the Climatol web page (http://www.climatol.eu/).

2.2.1 Data preparation

The data to be homogenized in Climatol must be provided in a predefined format. Climatol requires two input text files, one containing all the data (with extension “dat”) and another containing coordinates, elevation above sea level, station numbers and the station names (with extension “est”) in the same order as the data file. All the data must be present for the entire study period, and thus missing values are marked with “NA”.

[1] A candidate series is the series being tested for inhomogeneities, and the reference series are the neighbouring series to the candidate series.

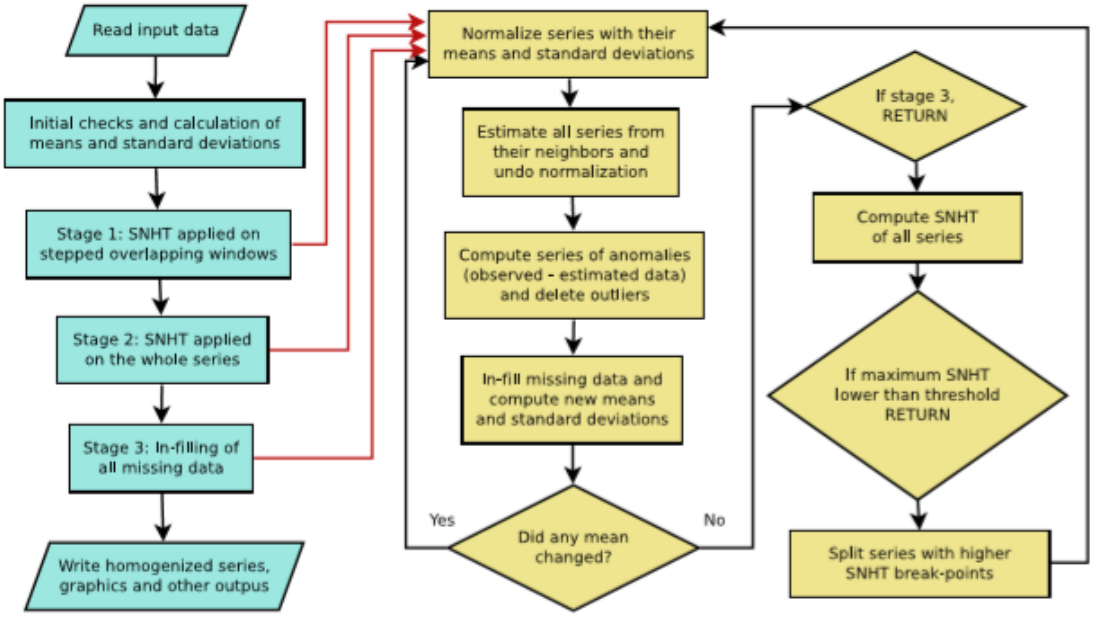

Figure 2: Tasks flow-chart of the Climatol package with its nested iterative processes (Guijarro, 2018). Red arrows show the progress from the main process (in blue) to the secondary one (in yellow). Shapes refer as follows: Rectangles (processes), parallelograms (input/output data), and diamonds (conditional processes).

2.2.2 Procedure and flow chart

Fig. 2 presents the homogenization procedure in Climatol. After reading the input data, initial checks are performed on the data, including calculation of means and standard deviation. Three stages then follow:

1. Detection of inhomogeneities by applying SNHT on stepped overlapping windows, until all series appear homogeneous
2. Detection of breaks using SNHT on the whole series
3. In-filling of all missing values using the weighted ratios of neighboring series, hence generating the final homogenous series

The homogeneity testing is done in two steps, first on overlapping stepped windows (stage 1) and then on the whole series (stage 2), in order to better handle multiple inhomogeneities in a series.

The homogenization outputs from Climatol are delivered in R binary format, containing the original and homogenized series, a collection of diagnostic graphics, three text files including one with a log of all the processing outputs and a list of corrected outliers and breaks.

The final step is the validation of the homogenized data, which entails critical evaluation of the homogenization method or process and to review the homogenized

data. All statistical analyses are connected with uncertainties, and therefore perfection is never achieved no matter how well the data are homogenized. Some residual inhomogeneity may still remain in the adjusted series, but the results give the best possible estimate. It is important to review each series to ascertain whether the new homogenized values make sense. Spatial coherence of the temporal evolution of the series, as well as comparison of the adjustment series to the known changes in the network can be useful when dealing with a full homogenized dataset.

2.2.3 Normalization

The SNHT method has the advantage that it allows data from nearby stations to be used even when there is no common period of observation. This therefore enables use of short series that would have otherwise been disregarded. To counter the irregularity of the observation periods, Climatol begins by normalizing all the original data and computing a reference series for each candidate series by averaging up to ten data series (if available) at every time step in the detection stages and four data series during the final series reconstruction. The user can change these numbers of reference series.

Climatol offers three types of data normalization using the most appropriate ratios or differences depending on the climatological variable:

1. deviations from the mean (subtracting the mean)
2. ratios to the mean (dividing by the mean) - only for means greater than 1
3. standardization (subtract the mean and divide by the sample standard deviation)

Ratios to normal climatological values (2) are suitable for climate variables that have a natural zero lower limit with a highly skewed (L-shaped) probability distribution, which is mostly the case for precipitation and wind speed. Standardization (3) or even (1) are more suitable to near-normal distributed variables such as temperature and pressure.

The default normalization option in Climatol is the standardization method (3) where *std*=3. The user has to choose the most appropriate normalization technique depending on the climate variable.

Estimations of means and standard deviations of the complete normalized time series (including missing values) are not computed for the whole study period if the time series is not complete. A nested iterative approach is thus used to estimate these statistics. Climatol first computes these statistical parameters from all available data in each time series and, after filling in the missing values, recomputes means and standard deviations. Then, using these new means and standard deviations, the series are re-normalized and missing data estimation is performed. The procedure is repeated until the maximum change between means of any data item in consecutive iterations becomes less than a given threshold (half of the data precision, defined by the number of decimals). The maximum number of iterations when computing the means is set to 999 by default.

Every term of the complete normalized raw data can then be constructed using an

weighted average of a prescribed number of normalized reference series (the default is up to ten series in stage 1 and 2, and up to four in stage 3, but these numbers can be changed by the user in the argument *nref* in the *homogen* function). No weights are applied to the series constructed in stages 1 and 2, because nearby series can still contain inhomogeneities. The weighting is applied in the final reconstruction of all series from the homogeneous sub-periods (stage 3). The reference series can be weighted by the same plain average or by an inverse function of the distance d_j. The weight function w_j is given by:

$$w_j = \frac{1}{1 + d_j^2 / h^2}$$

where d_j is the distance between the stations and h is the distance at which the weight becomes half that of a station placed at the same location of the candidate series. By default, the term h is set to 100 km in the third stage, but this can be changed by the user in the argument *wd*. It should be noted that when working to obtain climate normals (like in our case) the variance adjustment will have no importance, while they can be very crucial if deriving an extreme value return period in the series.

Finally, Climatol generates the final homogeneous series by filling in all missing data (including all the data removed in the outlier detection and break detection) by replacing them with estimated values of neighboring stations. The estimated series are also used to compute a series of anomalies (difference between normalized observed data and Climatol estimations) and calculate root mean square errors (RMSE) of the Climatol estimations, which can serve to compute confidence intervals for the homogenized series. The series of anomalies are computed for the detection of outliers and shifts in the mean (break detection).

2.2.4 Threshold for the SNHT test statistic

The SNHT test statistic is the measure for inhomogeneity in a series: The lower the maximum SNHT value is in a series, the higher the homogeneity of the series. Climatol computes SNHT values for all series before retaining the maximum SNHT values for each series. The series with maximum SNHT values higher than a set threshold are split into two sub-series at the point of the maximum SNHT value (as long as no reference series has been split in the same iteration with a similar value). The sub-series are then tested again and the procedure is repeated until the maximum SNHT values of the sub-series are below the set threshold. This is the part of the procedure called the “stepped overlapping windows” procedure. After all breaks in the stepped overlapping windows procedure are detected, the test is applied to the whole series, where further breaks could be detected.

The user has the option to adjust the threshold value and set different thresholds for the two procedures - one for the stepped overlapping windows (*snht1*) and one for the whole series (*snht2*). The default values are *snht1=snht2=25*, but the most appropriate

values will depend on the parameter, time resolution and on how many series are tested. No SNHT analysis will be performed if the threshold is set to zero.

The default values in Climatol are mostly appropriate for monthly temperature series, and the user documentation of Climatol recommends using the histograms from the exploratory run to find the optimal threshold values for data sets of other parameters and time resolutions, see Fig. 3 and Fig. 4.

2.3 Application of Climatol

In this study, after reading in the data, Climatol was run in exploratory mode with its default values for initial analysis of the original data. In essence, the first two detection stages of homogenization are skipped in the exploratory tests and only the anomalies of all the original series are shown. The results were then used to set and adjust the default threshold values. Precipitation is a zero-limited variable with a skewed probability distribution, thus Climatol was applied using the normal ratio normalization (*std*=2) and the graphical parameter set to four (*gp*=4), so that resulting outputs are of running annual totals (instead of means), which is better when working with precipitation data. The default thresholds were maintained for weights (*wd*) and number of references (*nref*) which were presumed optimal for the final purpose of this study. The diagnostic outputs from the exploratory stage were used for quality control and to verify that there were no abnormal features in the data.

2.3.1 Outlier detection

The series of normalized anomalies is used for outlier detection. The default threshold for outlier tolerance is set to ±5 standard deviations, and so the original data points outside this interval are deleted. This threshold was adjusted in this study to ensure that flagged outlying values were not excluded purely because of their extremeness. Precipitation is a variable with large variation, especially in Norway where topography has a large influence, and where heavy rainfall events connected to convective storms occur frequently in summer. A low outlier threshold gives an increased risk of removing legitimate observations that are due to natural variations.

Fig. 3 shows the histogram of the normalized anomalies grouped by the number of standard deviations. The default threshold for outliers (*dz.max*=5) proved to be too low, giving a list of 570 outliers. To examine a more suitable threshold for this study's dataset, the outliers with the highest anomalies (standard deviation > 10) were inspected. These potential outliers were inspected by looking at daily values and comparing them to neighboring data series. Most of the potential outliers turned out to be legitimate measurements. Some were a result of data entry error or processing error and were corrected. Because the potential outliers seemed to be legitimate observations,

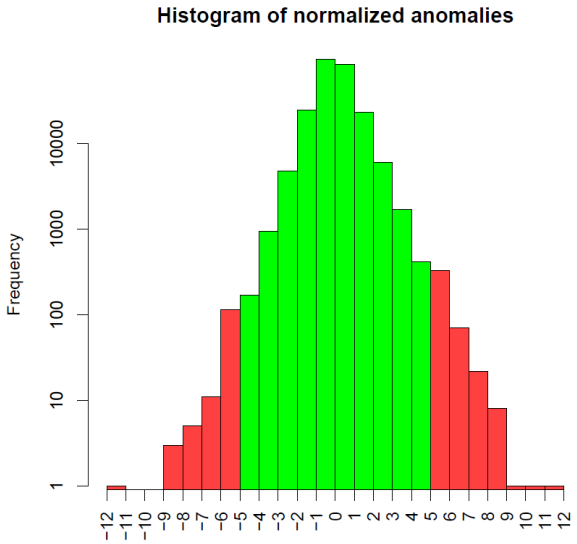

Figure 3: Histogram of normalized anomalies from the exploratory mode run. The x-axis gives standard deviations. The red bars are anomalies outside the default threshold of ±5 standard deviations.

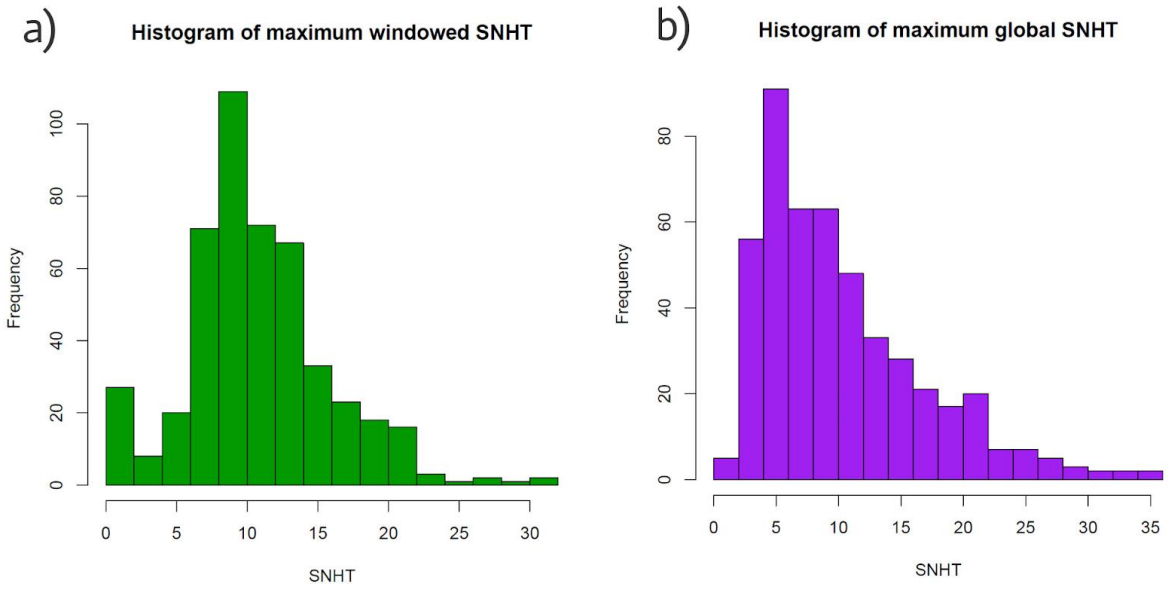

Figure 4: Histogram from the exploratory mode run of maximum SNHT values in the overlapping windows procedure (left) and in the whole series (right).

a high threshold of ±13 standard deviations was chosen, so that none of the natural variability in the series was masked or lost.

2.3.2 SNHT thresholds

Histograms of maximum SNHT are used to determine the most suitable detection threshold of changes in the mean of the series. The histogram of the maximum SNHT values from the stepped overlapping windowed procedure is used to set the value for *snht1*, and the histogram of the maximum global SNHT, that is, for the entire series, is used to set *snht2*, see Fig. 4. Generally, the histogram should show a high frequency of low SNHT values corresponding to fairly homogeneous series and one or more secondary groups of bars with higher SNHT values due to inhomogeneous cases. It could then be easy to set a threshold (SNHT) value between them for the detection stages. This is however challenging to set, especially when processing lower numbers of series, as frequency bars can be separated by several gaps or no gaps at all.

Determining the most suitable SNHT value for this study included visualization of the histograms of maximum SNHT, Fig. 4, and those from different runs where the SNHT value was varied. The assessment was conducted on the results from a run of all the 370 precipitation stations and on separate runs on five smaller region networks in Norway (Eastern Norway, Rogaland, Western Norway, Trøndelag and Northern Norway).

It was not straightforward choosing the most appropriate thresholds from the histograms, Fig. 4. However, after careful consideration, setting *snht1=snht2=22* seemed reasonable as there is visibly a secondary group of bars with a clear minimum after the SNHT value of 22. The singularity plot of station numbers with respect to their final RMSE and maximum SNHT values, Fig. 5, also showed that most of the series analysed were in a test statistic range (SNHT) of 20, and with RMSE between 10 and 40.

Other threshold values were also tested (*snht1=snht2*=25, *snht1=snht2*=20, *snht1*=15 and *snht2*=25, *snht1*=20 and *snht2*=30). As expected, tests with higher thresholds gave fewer detected breaks and tests with lower thresholds gave more breaks. The lower thresholds also gave more “outlier breaks", that is, breaks occurring within a short time period of each other (a year or two apart or sometimes within the same year) caused by either especially high or low precipitation amounts. These are not actual homogeneity breaks, but a result of outliers. These test runs showed that one would have to choose a threshold low enough to include as many valid breaks as possible, but high enough to exclude most of the outlier breaks and falsely detected breaks. This supported the choice of 22 as a threshold. Results from the study on five different regions in Norway further supported the choice.

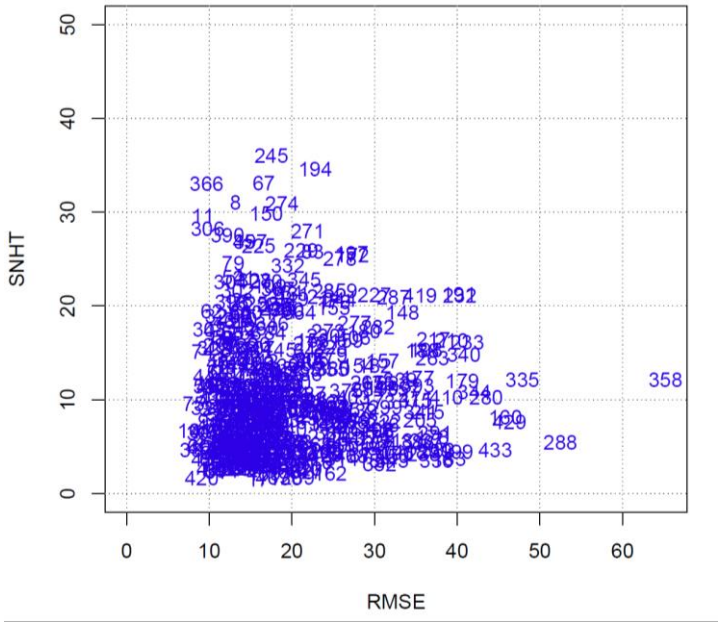

Figure 5: Singularity plot of maximum SNHT values versus RMSE from the exploratory run in Climatol for all of the 370 precipitation series.

2.3.3 Break detection and metadata

As previously highlighted, three stages follow the initial exploratory analysis stage:

1. Detection of inhomogeneities by applying the SNHT (using the threshold set by the argument *snht1*) on stepped overlapping windows, splitting the most inhomogeneous series by the detected break points, and repeating the process until all series appear homogeneous
2. As in 1., but applying the SNHT (using the threshold set by the argument *snht2*) to the entire series (i.e. 1961–2018)
3. Generation of the final homogeneous series by filling all missing data by weighted ratios of nearby stations in the homogeneous sub-series

The detected breaks in the analysis were carefully examined against available metadata. While the results in Climatol provided strong evidence about the inhomogeneities in the series, metadata indicates the cause of an inhomogeneity, and helps determine the exact date of the inhomogeneity. The metadata was obtained digitally from MET Norway's database. The paper archive of station files at MET Norway was also used as a source. The use of metadata is a time consuming process, but adds great value and confidence to the homogenization results. The detected breaks in the Swedish and Finnish series could not be verified because metadata was not available in this analysis.

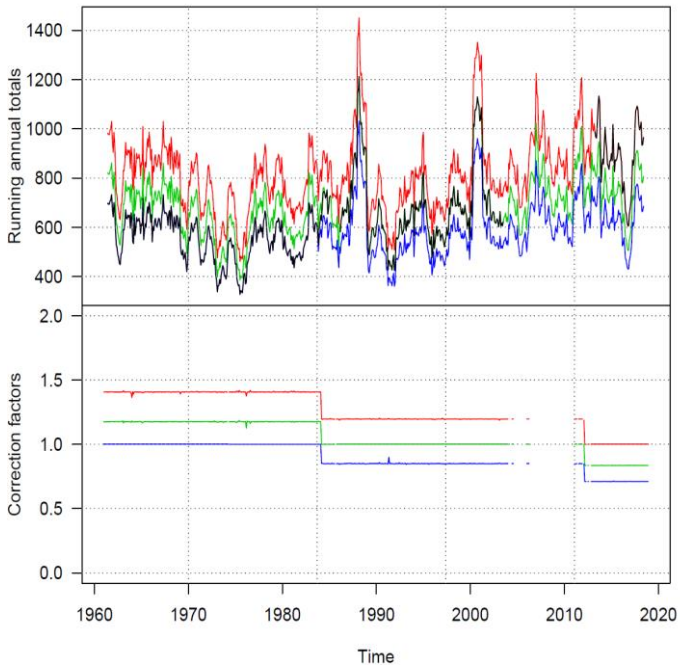

Figure 6: Example for 29350 Uvdal kraftverk of series reconstruction (top) and correction factors (bottom). Black line is the original series. Red series is adjusted using the latest homogeneous sub-period of the series (2012-2018, the period after the second break in the series) as a base level, i.e. adjusting the rest of the series relative to this level. Green line uses the middle sub-period (1984-2012, period between first and second break) as a base level, and blue uses the first sub-period (1961-1984, period before first break) as a base level.

It should be noted that in the presence of metadata, the break file in Climatol can be conveniently edited to adjust the dates of the detected break-points to match the metadata and also to remove unverified detected breaks before running the homogenization function (*homogen*) again with the added parameter *metad*=TRUE.

The dates of the accepted breaks were adjusted to match those of the reported metadata (if they did not match). In some instances Climatol's date was used when the exact dates of change were not available in the station files, for example when metadata reports a relocation but only specifies the year and not the exact date of the relocation. Climatol's suggested date was also used in cases when there were several changes in the station around the time of the detected break.

Criteria for inhomogeneities

The criteria for accepting detected breaks were quite strict. All but one of the accepted breaks were supported by metadata. For the inhomogeneity to be confirmed, Climatol's detected break-point had to be within five years of the metadata explaining the break. The break that was accepted without metadata supporting it was accepted because of the very high SNHT value of 102.9. Detected breaks within the first and last five years of

the series were rejected (two exceptions were however made, for the case of 52860 Takle and 60800 Ørskog as their inhomogeneities could be explained with obvious reasons and were four years from the end of the series. These breaks should be re-evaluated again later when there are more data points on each side of the breaks). Close breaks, especially within five years of each other, were assessed carefully, and weight was placed on the break point with metadata (or the most obvious or dominant reason for a break). In addition, outlier breaks were rejected.

Break adjustments

Climatol provides the option of different reconstructions of the homogenized series, see Fig. 6. The homogenized output series can be reconstructed from the last sub-period, i.e. adjusted backwards from the last homogeneous sub-period. This option is good for climate monitoring and was the option used in this study. The user can however choose to use output series reconstructed from other sub-periods as well.

The precipitation series are adjusted with a constant annual correction factor in each sub-period (Climatol does not give the option of monthly adjustment factors for precipitation, only annual adjustment factors are available), see lower panel in Fig. 6. The "spikes" are due to outlier rejection.

3 Results

3.1 Exploratory mode results

Fig. 7a shows the correlogram of the monthly correlations between stations. The figure shows relatively high correlations (> 0.8) for stations located within approximately 50 km distance of each other. The correlation coefficient is then seen to decrease rapidly with distance reaching negative values in stations located up to a distance of ca. 100 km. This is no surprise considering the varied topography in Norway that includes orographic discontinuities that may give opposite precipitation regimes. The mountainous areas near the coast receive the highest precipitation amount (annual sum > 5000 mm) while the more continental parts of the country are much drier with annual sums as low as 300 mm.

The map of stations in Fig. 7b shows the cluster analysis of the precipitation series, giving a sense of the different precipitation regions in Norway. Climatol limits the cluster analysis to a maximum 100 stations as a default. This is to avoid time-consuming processing of large correlation matrices, and also avoid very dense graphics that are hard to read. However, this can be changed by the user to include all series in the analysis (using the argument *nclust* in the *homogen* function). In addition, Climatol restricts the number of clusters to a maximum of nine. The cluster analysis shows precipitation regions similar to those found by Hanssen-Bauer and Førland (1998) who used comparative trend analysis on 100 precipitation series in the period 1896-1997 to define thirteen precipitation regions. The differences in the precipitation regions between this analysis and that of Hanssen-Bauer and Førland are mostly due to the restriction in Climatol of nine clusters; also, the different series and time-periods may have influenced the result.

3.2 Homogenization results

Climatol detected 121 breaks in the Norwegian precipitation series. After conferring with metadata, 90 of these breaks were accepted. Thus, 81 (25 %) of the 325 Norwegian precipitation series were classified as inhomogeneous. Climatol detected 16 breaks in

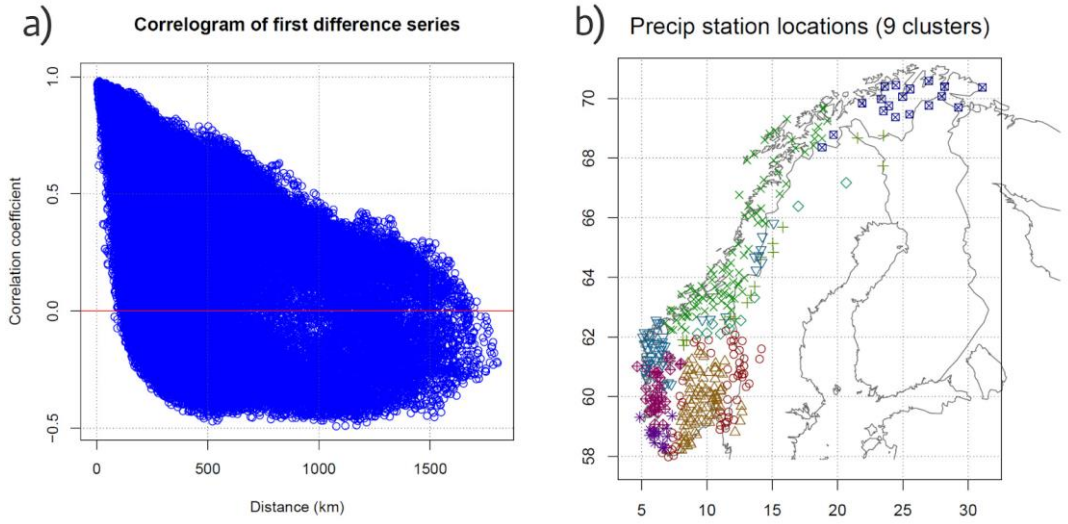

Figure 7: Correlogram (left) and spatial distribution of clustered stations (right) of the precipitation series. All 370 series were included in the correlogram and cluster analysis.

the Swedish precipitation series used as reference series. All breaks in the Swedish series were accepted since metadata for these series were not available.

Climatol detected no inhomogeneity in 263 of the 370 series (including Swedish and Finnish series). After conferring with metadata and rejecting some of the breaks, 276 of the stations were classified as homogeneous (including Swedish and Finnish series).

Fig. 8 summarizes the number of breaks detected in the Norwegian precipitation series. Results from the run without using metadata for accepting breaks, upper panel in Fig. 8, show that the series with detected breaks had up to four breaks, but most had only a single break point. Looking at the number of breaks per year, a maximum number of breakpoints (nine breaks) were found in 2011. Further inspection showed that five of these breaks were outlier breaks. After the use of metadata to accept, reject and adjust the date of the breaks, the same summaries of detected breaks were made, see lower panel in Fig. 8. This shows the same pattern of one break per series being the most common. The split frequencies per year shows that there are more breaks in the last part of the period than in the first half (50 vs 40 breaks). This is not surprising as many and large changes have occurred in the Norwegian station network especially after the year 2000, and especially in regards to automation of stations.

3.2.1 29350 Uvdal kraftverk

An example of inhomogeneity detection with Climatol for 29350 Uvdal Kraftverk (in Southern Norway) series is shown in Fig. 9. The anomaly plots are from stage two in Climatol and the shift in the mean of the series is marked by a red vertical line. Fig. 9a illustrates the detection of a break in 2012, which has a SNHT value of 103. This is well

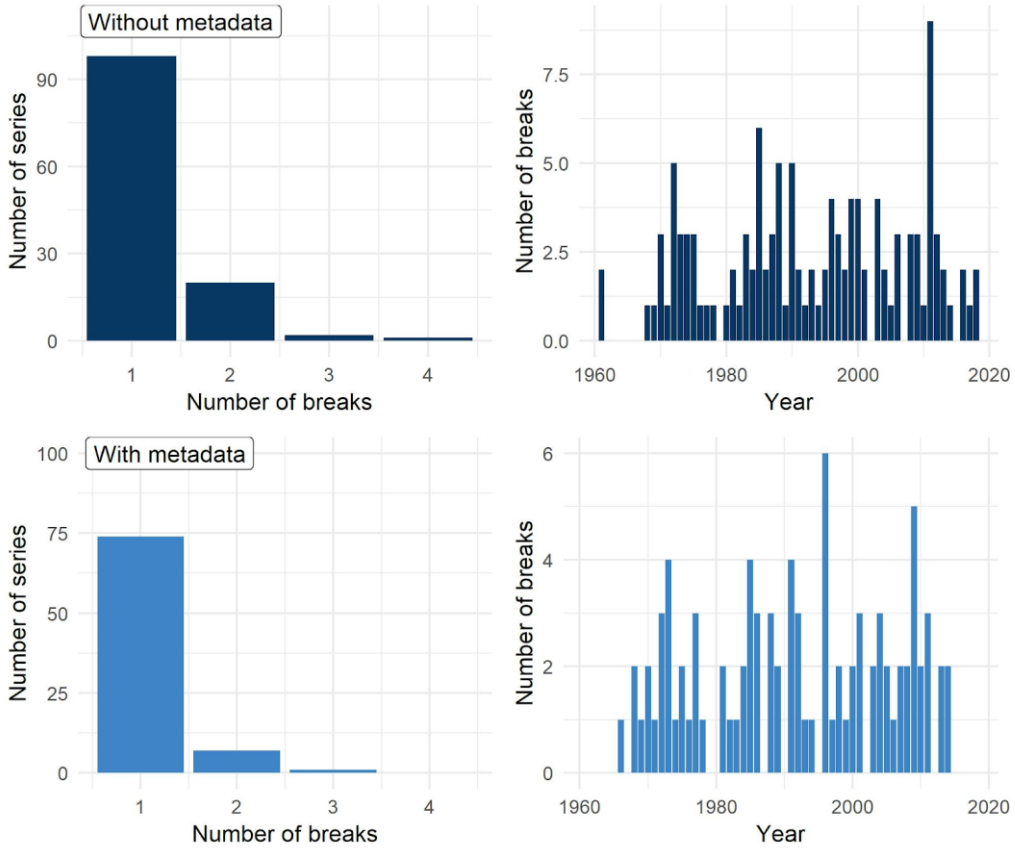

Figure 8: Number of breaks per series (right) and per year (left) for the Norwegian precipitation series. Upper panel shows results when accepting all detected breaks without using metadata. Lower panel shows results when using metadata as criteria for accepting breaks.

above the set SNHT threshold of 22, and the series is then split in two sub-series at the break point marked by the red line. The two sub-series are again tested for homogeneity in later iterations. A second break in 1984 was detected in the later iterations with a SNHT value of 50, Fig. 9b. After the break points in the series have been identified, the series is adjusted and missing data interpolated, Fig. 6.

The break in 2012 had a very large SNHT value of 103, and Climatol suggested a most probable date of break to March 2012. Metadata showed that an automated weather station was installed at the station in 2006 and ran parallel with the manual station. The manual measurements were the official measurements until February 2012 when the data from the automatic station became the official ones. February 2012 was therefore set as the date of break. The annual adjustment factor was 1.15, showing that the automatic precipitation gauge that was placed at the same spot as the manual gauge but slightly higher above ground and with a different wind-shield, had a gauge catch 15 % larger than the manual gauge.

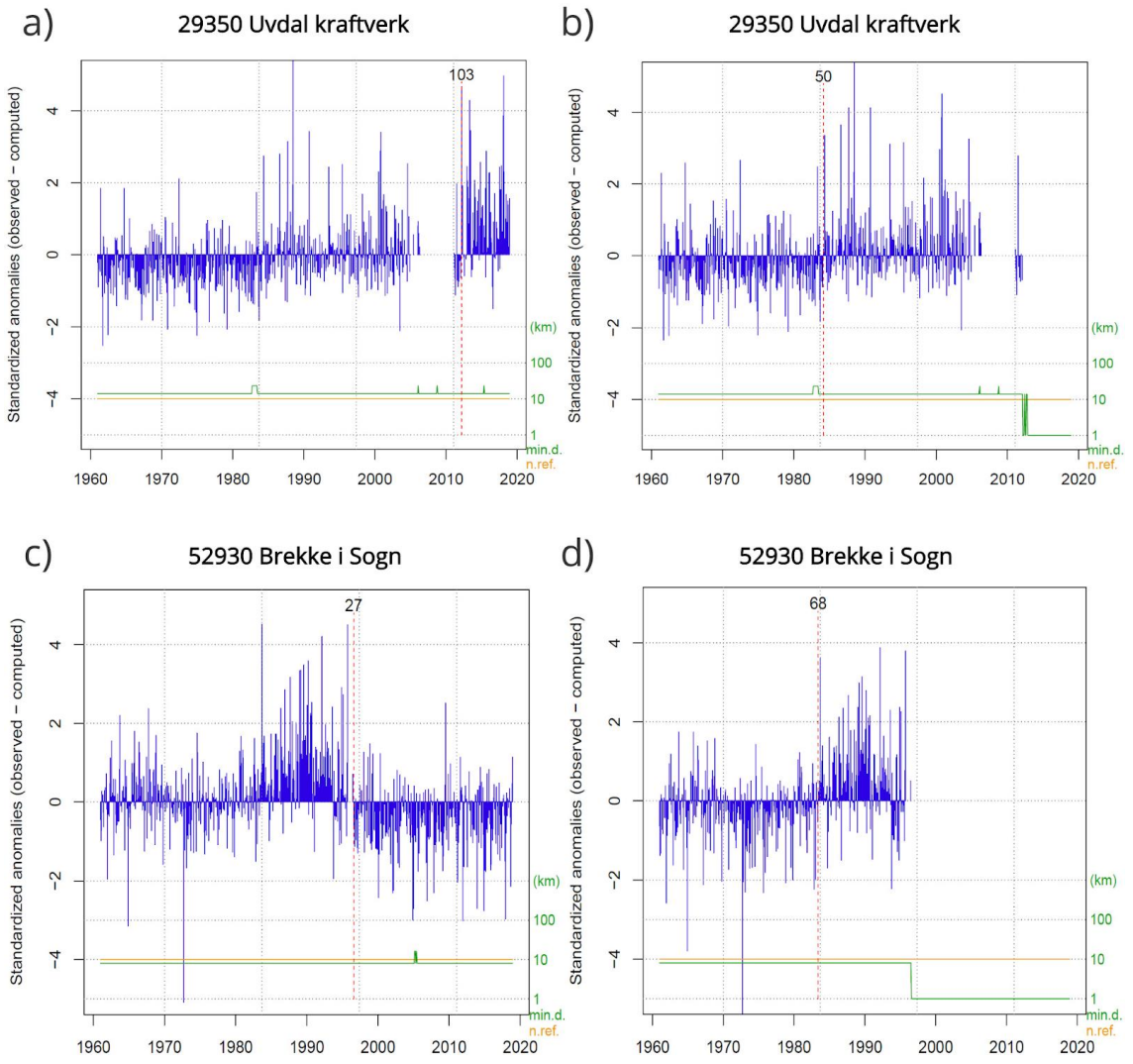

Figure. 9: Anomaly plots from Climatol, showing break detection results for 29350 Uvdal kraftverk (upper panel) and 52930 Brekke i Sogn (lower panel). Red dotted vertical line shows placement of the maximum SNHT value of the series. Number next to the red line is the maximum SNHT value. Orange line shows the number of reference stations and the green line shows the distance to the nearest neighbour station, both at each time step using the logarithmic scale. (a) First split in the Uvdal series in 1996. (b) Second split in the Uvdal series in 1983 at a later iteration. (c) First split in the Brekke i Sogn series in 2012. (d) Second split in Brekke i Sogn series in 1984 at a later iteration.

The break in 1984 had March 1984 as the most probable date of break in Climatol. Metadata showed that the series was merged with station 29310 Uvdal II, which was located 4 km east of Uvdal kraftverk, in October 1985. There was also a change of observer at Uvdal II in 1984, but this was not thought to be the main reason for the break. A relocation (i.e. merging) was considered a much more plausible explanation for the break, and October 1985 was therefore set as the date. The annual adjustment factor was 1.36, meaning that the gauge catch at Uvdal II was 36 % lower than the

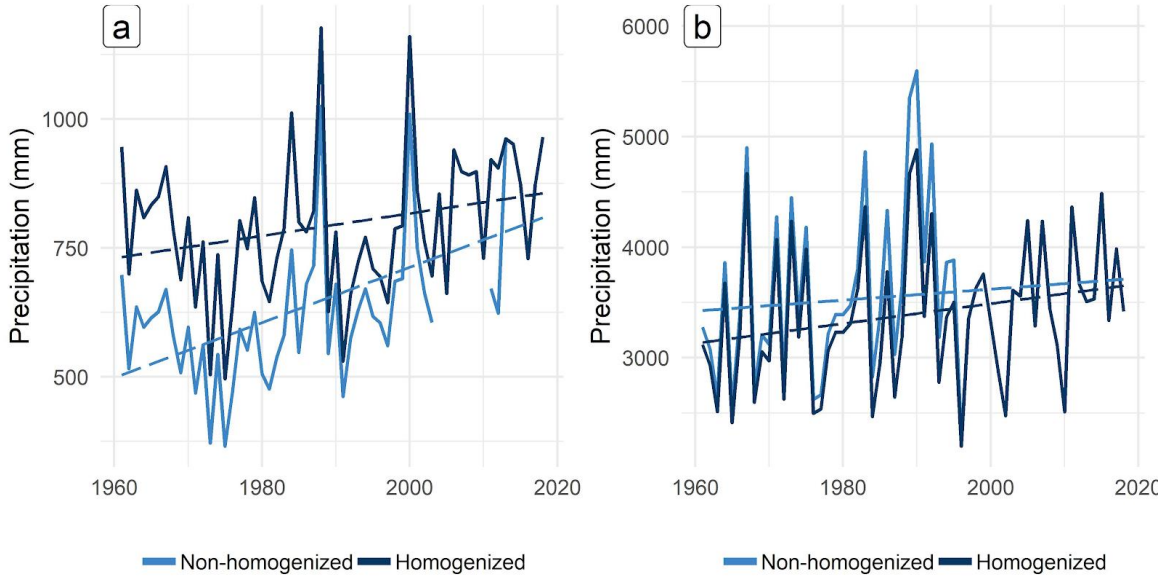

Figure 10: Homogenized and non-homogenized annual precipitation series with linear trend lines for (a) 29350 Uvdal kraftverk and (b) 52930 Brekke i Sogn.

gauge catch of the automatic gauge, and 21 % (36 % - 15 %) lower than the manual gauge at Uvdal kraftverk.

Metadata also showed two other changes at the station that potentially could have caused breaks. In 1991, the standard Norwegian rain gauge was replaced by a Swedish SHMI gauge. MET Norway has previously conducted parallel measurements and shown that there are usually only small differences between the two gauge types (less than ±3 % on a yearly basis, cf. Førland and Aune (1985b)), and so it is not surprising that this did not cause a break in the Uvdal kraftverk series. The rain gauge was located close to a forest. The vegetation south of the gauge was not kept down on a regular basis, but a few small trees near the gauge were removed in 1991. It was commented in the inspection report in 2007 that the vegetation had changed character since the station was established in 1985 and since the clearing of vegetation in 1991. These changes in the environment around the gauge were not large enough to cause a break.

Fig. 10a shows the inhomogeneous and the homogeneous annual series for Uvdal kraftverk. The earliest part of the series has been adjusted up to match the increased gauge catch that the change to an automatic rain gauge caused, and so the linear trend of the homogenized series is smaller than that of the inhomogeneous series (22 mm/decade for the homogenized series, 54 mm/decade for the inhomogeneous series).

3.2.2 52930 Brekke i Sogn

Another example of break detection and correction is shown in Fig. 9 for the station 52930 Brekke i Sogn (in Southwestern Norway). The anomaly plots show a detected break in the first iteration in 1996 with SNHT value of 27. Climatol suggested August 1996 as the most probable date of break. Metadata showed a relocation on 1 July 1996 that also included a new precipitation gauge and a new observer. There was also a new observer at the station in 1994. The relocation was considered to be the main reason for the break, and the date was set to July 1996. The adjustment factor was 0.87, implying that the new placement was more exposed to wind therefore making the gauge catch 13 % lower.

A second break was detected in a later iteration in 1983, with a SNHT value of 68. Climatol's suggested date of the break was June 1983. The metadata records showed a new observer in 1986. An inspection report in August 1984 commented that some trees south of the precipitation gauge had grown considerably and had probably given more shelter from the wind and hence increased the gauge catch. The changes in vegetation was set as the main reason for the break, and the date suggested by Climatol was accepted. The adjustment factor was 0.95, which means the gauge catch before 1983 was 5 % higher relative to the period after 1996. It also means the gauge catch in the period 1983-1996 was 8 % (13 % - 5 %) higher than that before 1983.

The homogenization analysis produced adjustments that resulted in a larger linear trend in the homogenized series than in the inhomogeneous series (50 mm/decade for the inhomogeneous series and 90 mm/decade for the homogenized series), Fig. 10b.

3.2.3 Main reasons for inhomogeneities

A total of 121 breaks were detected in the Norwegian precipitation series by Climatol. 90 of these breaks were accepted. Ten breaks were rejected because they were too close to the ends of the series (within the first and last five years of a series), 13 were outlier breaks, and the rest had either no or not convincing enough metadata supporting them.

The main reason for inhomogeneities was relocation, explaining 71 % of the breaks in the Norwegian precipitation series, Fig. 11. This includes both large relocations (>100 m) with, in some cases, changes in equipment and new observers, and relocations of just a few meters. Large relocations can cause inhomogeneities when there are differences in precipitation conditions between the new and old location. A typical example of this is that precipitation in coastal areas of Western Norway increases by about 4 % per km distance from the coast (Førland 1979), an effect that is explained by the orographic lift of the moist air by the mountains. An example of this is station 55820 Fjærland Bremuseet that was relocated about 1.5 km closer to the fjord, resulting in a decrease in annual precipitation by 9 %.

Small relocations may cause breaks of homogeneity when the move leads to a change in the exposure of the precipitation gauge. Precipitation, and especially solid precipitation, is sensitive to changes in wind speed. As an example, a change in wind speed from 15

m/s to 10 m/s can increase the gauge catch for dry snow by about 30 % (Førland and Aune, 1985a). Therefore, small changes in exposure, that is, changes in wind conditions, can cause changes in gauge catch. In 70850 Snåsa Kjevlia, for example, a 30 m relocation of the precipitation gauge caused an increase of annual precipitation by 10 %.

Automation explained 12 % of the accepted breaks. Automation of a station includes changes in gauge and windscreen, measurement frequency and often a small or large relocation, which in turn may lead to changed exposure. In general automation leads to a reduced gauge catch in the Norwegian precipitation series, see section 3.2.4.

Change in the close environment surrounding the precipitation gauge caused almost 7 % of the breaks. Such changes include both gradual and sudden changes. It can be slow growing vegetation that over time gives a more sheltered environment or sudden changes such as new buildings or removal of vegetation. All of these changes can influence the wind exposure and so cause differences in gauge catch.

Change of observer is set as the main reason for about 4 % of the accepted breaks. Measurements and observations should ideally be independent of the observer, but there may be cases where a change of observer leads to changes in routines, which in turn may lead to inhomogeneities. In half of the breaks with change of observer as a reason, there were some additional changes around the same time as the change of observer. Station 12800 Mesna-Tyria changed its precipitation gauge from Norwegian to Swedish in the same year as the new observer started. But because parallel measurements in previous studies have shown that changes in the precipitation gauges only lead to small changes in precipitation, of less than ± 3 % (Førland and Aune 1985b), a new observer was set as the main reason rather than change in equipment. At the station 20520 Lunner a note was made during an inspection that some trees were removed a few years prior to the change of observer. However, because the change of observer coincided with the suggested date of change, and the tree removal had no date, a new observer was set as the main reason. It should also be noted that the metadata archive is incomplete, and so there may have been other changes at the station that were just never recorded.

Other reasons explained about 4 % of the accepted breaks. These reasons include irregular observations, cases of new equipment and in most cases; several changes happened at once, e.g. the station 44520 Helland i Gjesdal that was equipped with a new gauge at the same time as change of observer, in addition to a possible vegetation change around the gauge.

One break was accepted even though there were no known reasons that could explain the break. There were strict criteria for accepting breaks, and the break at station 89650 Innset i Bardu was only accepted because of its very large SNHT value of 102.9. There were notes from inspections of irregular observation practices and possible changes in the surrounding vegetation, but nothing specific enough to be set as an explanation.

It should again be noted that the metadata may not be complete and also that the process of collecting and going through all metadata is very time consuming, and so with more time one might be able to find good enough reasons for more of the detected breaks.

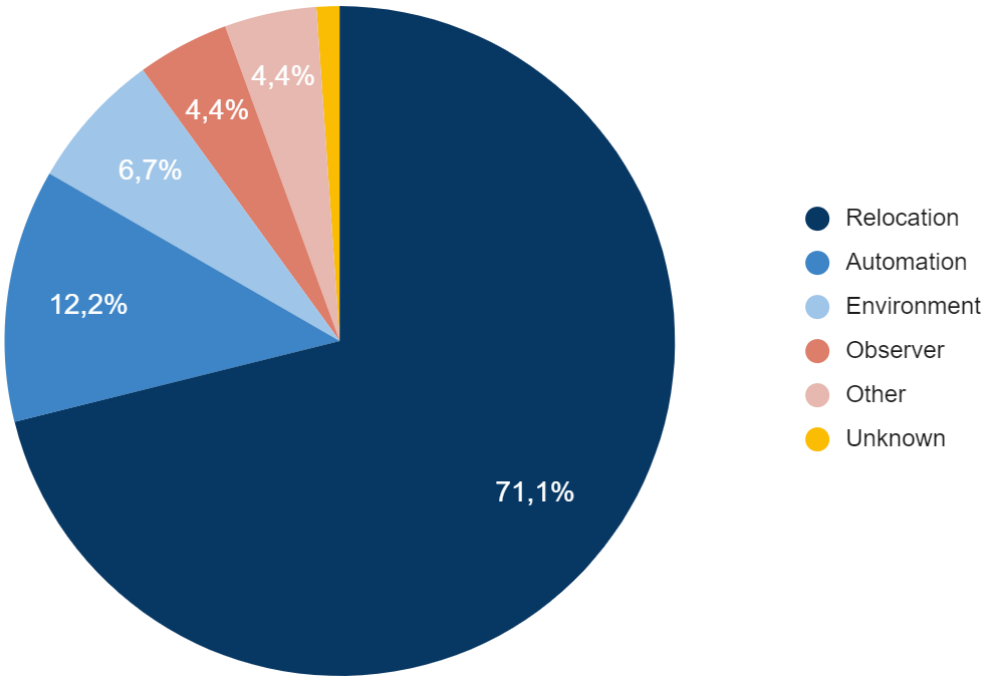

Figure 11: Reasons for inhomogeneities in the Norwegian precipitation series. They include relocation of the rain gauge, automation of the station, environmental changes, change of observer, other and unknown reasons.

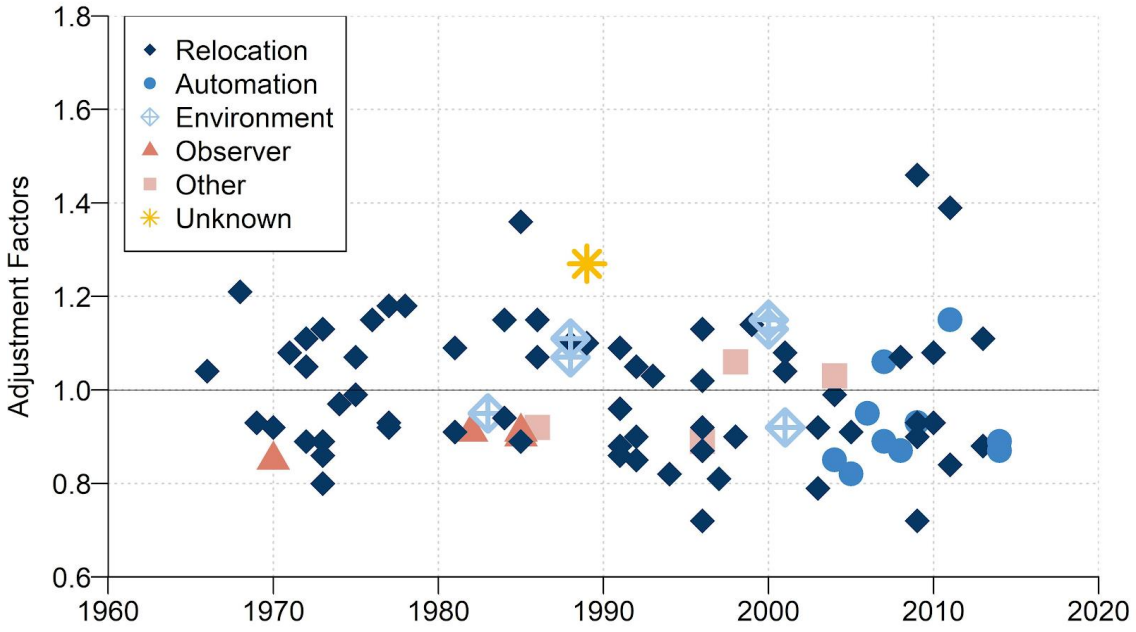

Figure 12: Annual adjustment factors for all the detected inhomogeneities plotted against time grouped by their causes.

3.2.4 Analysis of inhomogeneities

Fig. 12 presents the annual adjustment factors (AFs) for all detected inhomogeneities in the Norwegian precipitation series, sorted by its causes. The distribution of AFs is quite symmetrical and values vary between 0.72 and 1.46. 56 % of all the adjusted inhomogeneities had AFs below one, giving a general decrease in the mean measured precipitation in the country. The different causes for breaks show somewhat different patterns.

Relocation

Relocations caused the largest annual adjustments, with AFs between 0.72 and 1.46. Relocation may cause breaks due to differences in either exposure or precipitation conditions between the two sites. The AFs are quite symmetrical around 1 with the mean value 1.008, which shows that there is no systematic tendency in the relocation AFs. The test results further showed that there is no relationship between large relocations causing significant breaks with high AFs and small relocations causing insignificant breaks with lower AFs. Some large relocations of several kilometres led to very minor changes in the precipitation (break with just 1 % adjustment, or no break at all) while other small relocations of only a few meters led to major changes in precipitation with adjustments of 10 % or more and vice versa. This illustrates that significant changes can be expected regardless of how far the precipitation gauge is moved; it all depends on the local conditions at the site. This can be further exemplified by station 71810 Åfjord Momyr that had a 2 km move with a resulting AF of only 1 %. A second relocation of only a few metres at the same station caused a 10 % increase in precipitation.

New observer

Change of observer caused AFs in the interval 0.85-0.91 with a mean value of 0.89. Changes in observer as mentioned above should ideally not influence precipitation measurements, but it may in some cases still cause changes in observation practices. The four accepted breaks with change of observer as the main reason all gave adjustments in the same direction, with an average of 11 % decrease in annual precipitation after the change.

Environmental change

Changes in the local site environment caused inhomogeneities with AFs in the interval 0.92 -1.15 with mean value 1.06. Two of the breaks with environmental change as the main reason resulted in a lower gauge catch, while four breaks gave an increased gauge catch. This implies that most of the changes in the environment increased sheltering of the gauge, hence a 6 % increase in the annual precipitation after the change.

Automation

Station automation caused adjustments of the precipitation series in the interval 0.82 - 1.15 with a mean value of 0.93. This suggests that the majority of cases with automation resulted in a decrease in measured precipitation amount, with an average decrease of 7 % in annual precipitation. This is in accordance with previous parallel measurements between manual and automatic gauges conducted by MET Norway, where the general tendency is that the measured precipitation amount is lower with automatic gauges on mainland Norway (e.g. Nygård 2004). But this will of course vary depending on wind exposure, season and amount of precipitation as snow in addition to whether the manual gauge was equipped with a windscreen. In very wind exposed areas where a larger fraction of precipitation falls as snow, the automatic gauge may catch more precipitation than the manual gauge.

It is important to note that in most cases, the automation was coupled with a small or large relocation at the same time, and so the different precipitation conditions and wind exposure would also affect the AFs.

3.3 Effects of using metadata

While applying automated homogenization algorithms have been seen to give better results than user reliant algorithms (Venema et al. 2012), incorporating metadata to the statistically estimated breakpoint is often preferred. Most statistical algorithms usually identify inhomogeneities in climate series accurately, but are not able to determine their precise positions (Lindau & Venema, 2016). As mentioned above in chapter 2.3.3, strict guidelines for inhomogeneities were followed in this study to avoid over-adjusting the precipitation dataset. To analyze the effects of using metadata in the homogenization of the precipitation series, a comparison was made between the raw series, Climatol's automatically generated homogenized series and the homogenized series where metadata were used to verify breaks. The analysis was done for the 95 series with detected breaks, Fig. 13.

Looking at the long-term variations there is very little detectable difference between the two homogenized filtered anomaly series. The two homogenized series have very similar linear trends: 2.864 and 2.865 % per decade, and thus the difference induced by use of metadata is rather insignificant on a regional scale. The non-homogenized series exhibits a 1.8 % linear trend per decade.

When looking at larger scales and averaged data, the difference in result when using metadata and not using metadata is negligible. However, the differences can potentially be large when analyzing single series. Fig. 14 shows filtered values of the raw and homogenized series for 10600 Aursund. The Aursund series had four detected breaks. Two of the breaks occurred within two year of each other (September 1996 and October 1998), while the other two occurred within the same year (May and October 2011). In addition, each set of breaks had adjustment factors with opposite signs of each other. The breaks in 2011 were clear outlier breaks and were rejected. The 1996 and 1998 breaks were inspected more carefully. While a set of guidelines were followed in this

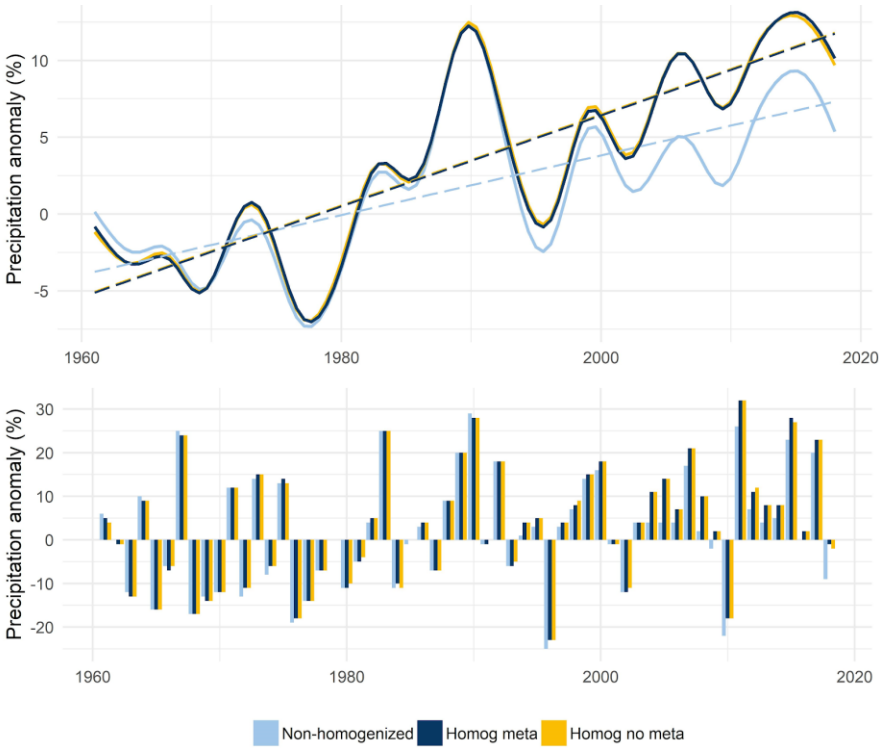

Figure 13: Comparison of non-homogenized series (light blue), the automatically generated homogenized series (yellow) and the homogenized series where metadata was used to verify breaks (dark blue). Lower panel shows the standardized anomaly series of the mean of all the 95 Norwegian annual precipitation series with detected breaks using 1961-1990 as reference period. In the upper panel, these series are filtered using a Gaussian density function to show precipitation variations on a five-year scale with linear trend lines.

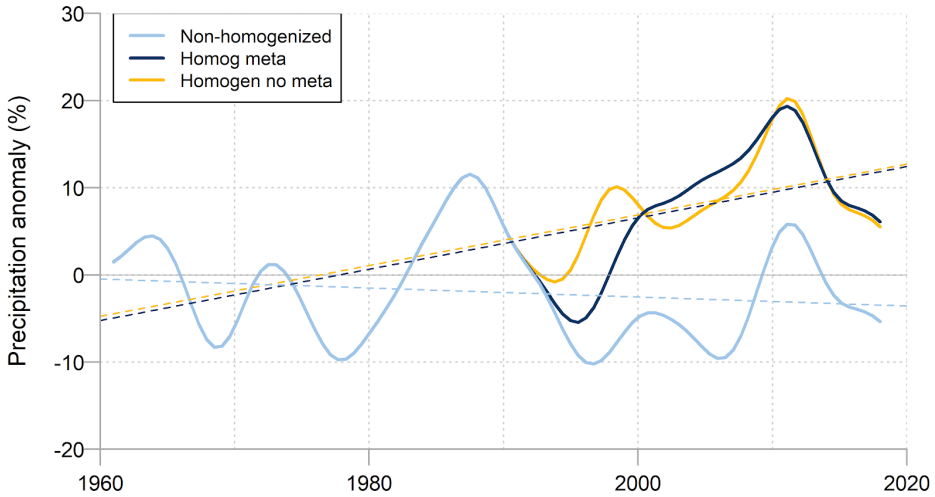

Figure 14: Comparison of non-homogenized series (light blue), the automatically generated homogenized series (yellow) and the homogenized series where metadata was used to verify breaks (dark blue) for 10600 Aursund with respect to 1961-1990 mean. The anomaly series has been filtered using a 5-year Gaussian density function. Linear trend lines are included.

study to avoid over-adjusting the dataset, a break in 1996 was still accepted because of the several changes recorded at the station around 1996-1998, including new equipment at the station and environmental changes around the precipitation gauge. These changes caused an AF of 0.89 implying that there was an 11 % decrease in annual measured precipitation at the station. When running Climatol again on the homogenized data set, no breaks were found in the Aursund series. Both homogenized series in Fig. 14 exhibit an increasing trend with time, in contrast to the raw series that has a decreasing trend. However, the temporal pattern in the two homogenized series are dissimilar, and shows that there can be pronounced differences in results when using metadata to accept and reject breaks. In this case, the automatic adjustment may have masked some of the natural variability in the series when adjusting the outlier breaks in 2011.

3.4 Impact of homogenization

To evaluate the impact and efficiency of homogenization on the precipitation series, a comparison was made between the non-homogenized and the homogenized series. The average of the annual and seasonal precipitation sums for all 325 Norwegian stations for both the non-homogenized and homogenized data was evaluated. The series were converted into standardized anomalies using 1961-1990 as the reference period and results are presented in Fig. 15.

The results of mean annual total precipitation for the whole Norwegian network do not show too large differences between non-homogenized and homogenized series. This is however not surprising as only about 25 % of series analyzed were adjusted. Precipitation is a variable with large spatial and temporal variance, which makes break detection harder than for other variables such as temperature. Breaks must be of a certain size to be noticeable over the general noise level, and thus many changes may not lead to detectable breaks. Nevertheless, some differences are seen where homogenization led to higher deviation from the 1961-1990 average. Values of annual anomalies in the non-homogenized series ranged from -23 to 27 %, while those of homogenized series ranged from -22 to 32 %.

Both non-homogenized and homogenized time series for the annual and seasonal series show increasing trends in the period 1961-2018 except in autumn where a decreasing trend is observed, Table 1. The 1961-1990 period is relatively wet in autumn compared to periods before and after. The new climate normal is therefore observed to be drier than the old normal for the majority of the series, especially in the northern and southwestern part of Norway. However, some areas in the north, northeast and southeast have seen an increase in autumn precipitation from the period 1961-1990 to 1991-2018, see also Fig. 17. The homogenized series have a higher trend compared to the non-homogenized series. 56 % of all the adjusted inhomogeneities had AFs, below 1. As a result, this net effect of the adjustments led to reduced precipitation values, especially in the earlier parts of the series, causing a more pronounced increasing trend in the homogenized series. The highest trend was observed in the winter series. The greatest difference in trend size before and after homogenization was observed in the annual

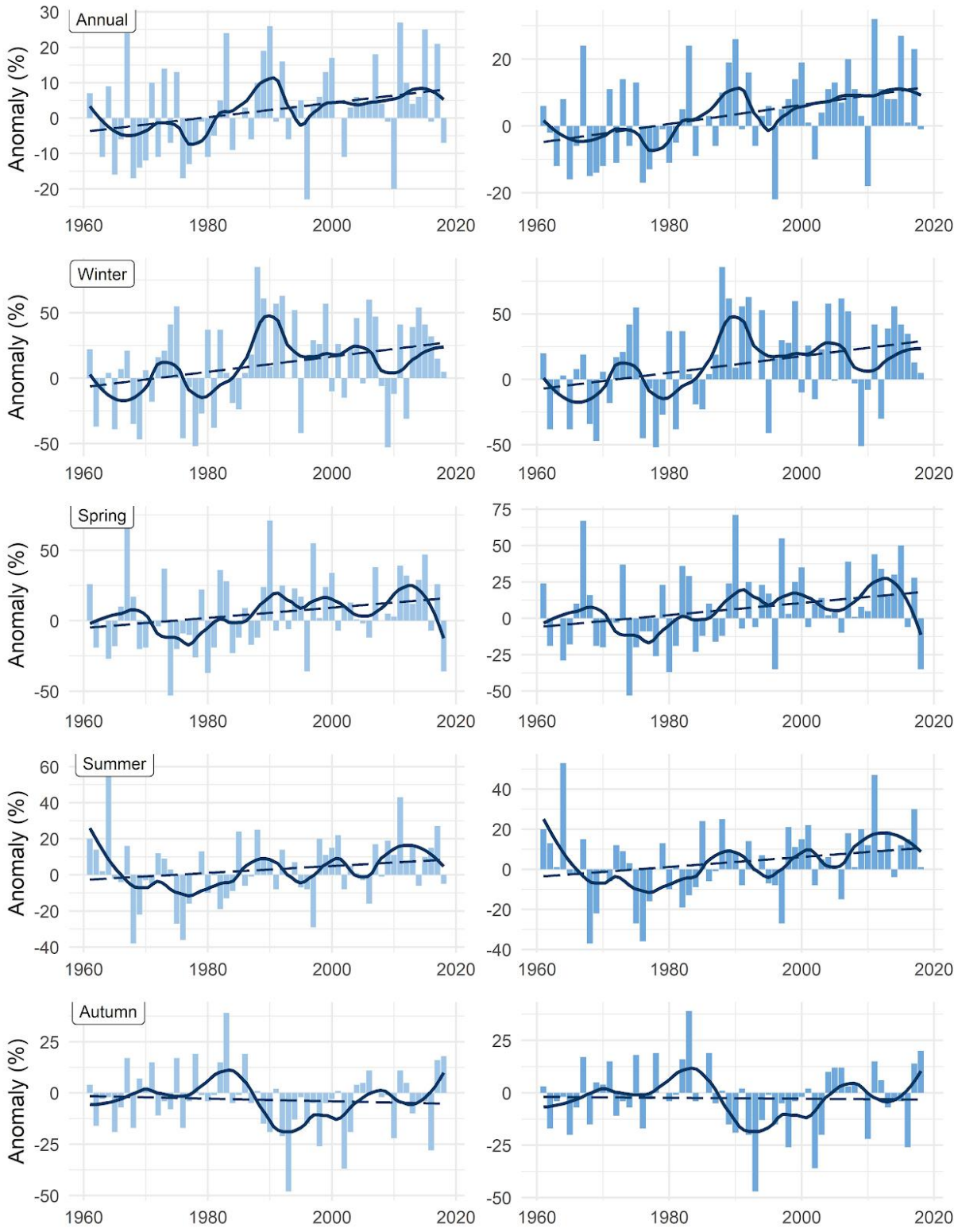

Figure 15: Standardized anomaly series for the Norwegian precipitation series before (left) and after (right) homogenization for annual and seasonal series using 1961-1990 as reference period. Linear trend lines and filtered series are also included.

series, where linear trends changed by 0.8 % per decade. Most of the increase in the precipitation series has been during the last 30 years.

To further understand the impact of homogenization on the precipitation series, the same calculations highlighted above were applied on some individual series representing different precipitation regions in Norway, Fig. 16. It should be noted that all series chosen had inhomogeneities that were adjusted. The range of anomalies with respect to the 1961-1990 reference period of the non-homogenized series is clearly wider than those of the homogenized series. Most represented series also show similar variability with time after homogenization. These results show that after homogenization, the spatial coherence of the temporal evolution of the series is better compared with the non-homogenized series. This proves that homogenization contributes to better temporal and spatial coherence of time series, while preserving the general statistical distribution of the raw time series.

Another comparison between the non-homogenized and homogenized series is presented in Fig. 17 where the difference between the two normal periods 1961-1990 and 1991-2020 is shown. The homogenized series exhibited smoother spatial patterns, meaning that the regional climate signal was well represented, with less local variations than in the maps based on the raw series. This is especially evident in the annual series.

In some regions, the ratio between the two normal periods changed from above 100 % to below after homogenization. The greatest variation in the homogenized series was in the southeastern region of Troms and Finnmark in Northern Norway where the highest decrease in both annual and seasonal precipitation was observed. From the map of annual series for example, the annual precipitation changed from over 140 % of the 1961-1990 mean before homogenization to under 100 % of the 1961-1990 mean after homogenization. This was also observed in the seasonal series. The results here are not surprising as most series with detected breaks in this region of Troms and Finnmark had large adjustment factors. The highest AF (1.46) was in 89940 Dividalen II that had a break in 2009, as a result of a 0.5 km relocation of the station that led to an increase in gauge catch. 89650 Innset i Bardu and 93900 Sihccajavri series with AFs of 1.27 and 1.39 respectively exhibited similar characteristics as that of Dividalen II. Most adjusted inhomogeneities in this region had large AFs above one; hence, the net effect of the adjustments led to increased precipitation values in the earlier parts of the series.

In conclusion, results based on the map after homogenization generally showed better regional coherence in comparison to the non-homogenized series. The homogeneous data are therefore more dependable in explaining the large-scale climate variations that should explain the change of "normal" climatologies.

Table 1: Linear trends (%/decade) of all annual and seasonal precipitation anomaly series 1961-2018 before and after homogenization.

	Annual	Winter	Spring	Summer	Autumn
Non-homogenized	2.05	5.85	3.63	1.92	-0.64
Homogenized	2.85	6.35	4.16	2.48	-0.22

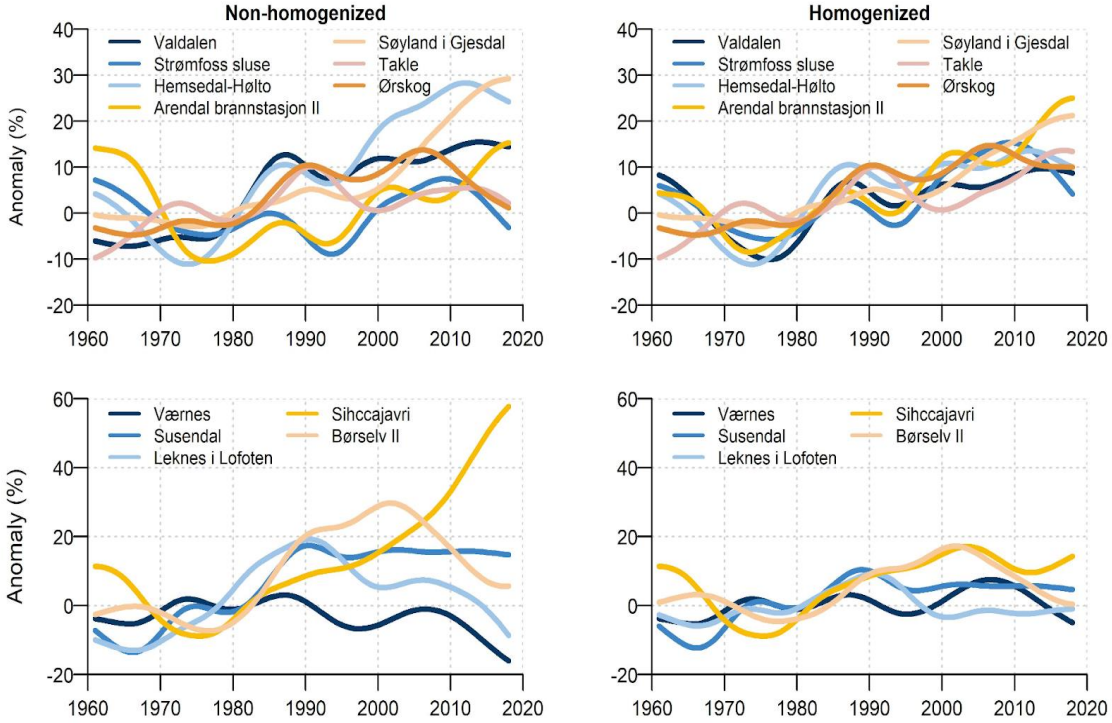

Figure 16: Deviation of the annual precipitation series in percent with respect to 1961-1990 mean for series in different climatic regions in Southern (upper panel) and Northern Norway (lower panel) before (left) and after (right) homogenization. The anomaly series have been filtered using a 10-year Gaussian density function.

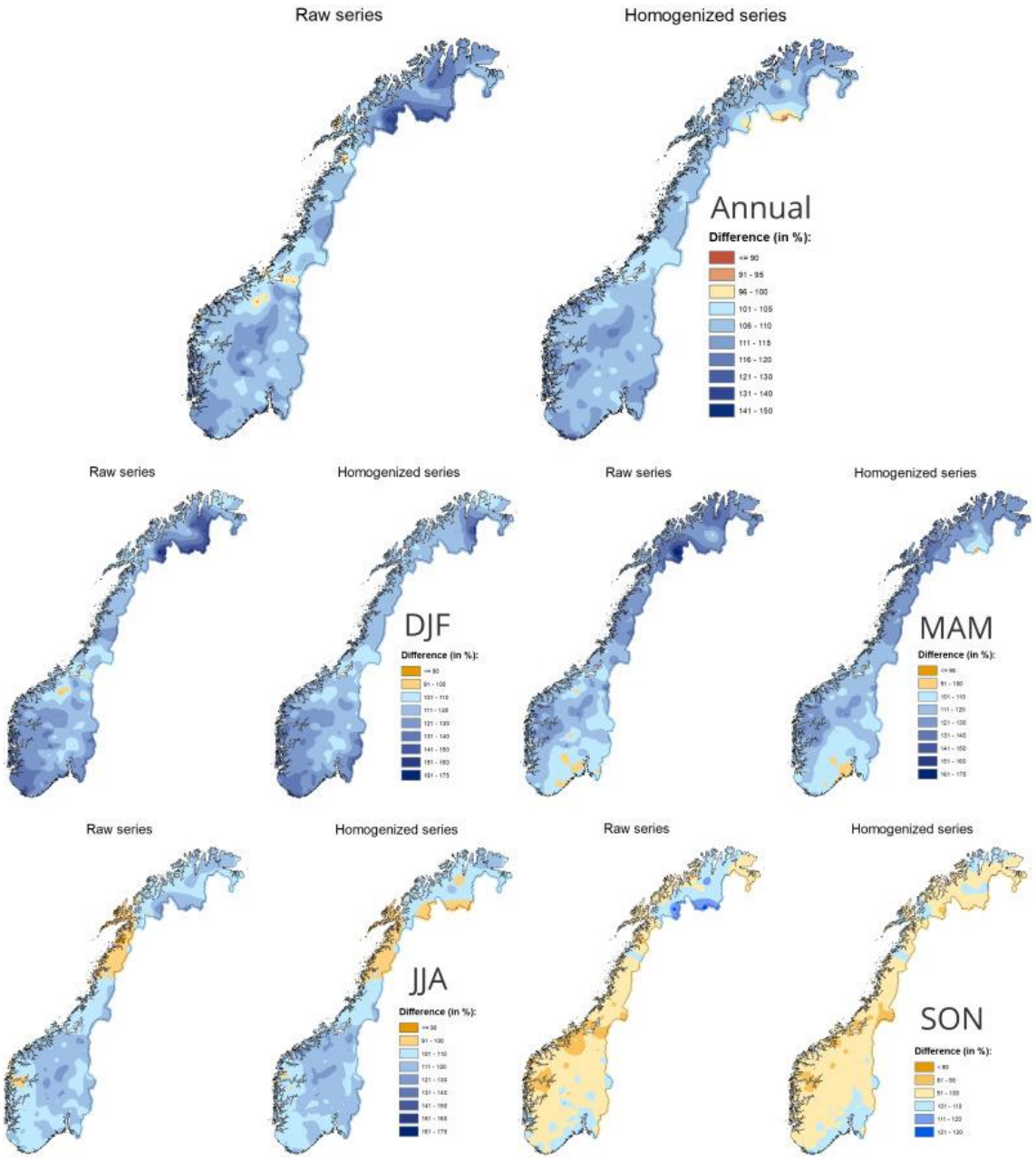

Figure 17: The ratio (in %) between the 1961-90 and 1991-2020 normal values based on raw and homogenized data series.

4 Summary and conclusion

The homogeneity analysis produced a 58-year long homogenous dataset for 325 monthly precipitation series, during the period 1961-2018. 370 series (including 44 from Sweden and one from Finland) from the ClimNorm precipitation dataset were used in the homogenization analysis. Application of Climatol homogenization method detected inhomogeneities in 95 (29 %) of the Norwegian precipitation series. A strict set of guidelines for inhomogeneity testing was followed to avoid over-adjusting of the dataset while still detecting as many real breaks as possible. Therefore, only 81 (25 %) of the series were classified as inhomogeneous after conferring with metadata and therefore adjusted. Precipitation is a variable with large spatial and temporal variance, which makes break detection harder than for other variables such as temperature. Breaks must be of a certain size to be noticeable over the general noise level, and thus many changes may not lead to detectable breaks.

The results of homogeneity testing showed that relocation of the precipitation gauge and automation were the main causes of inhomogeneities in the Norwegian series, explaining 71 % and 12 % respectively of all detected breaks. All but one of the accepted inhomogeneities could be confirmed with metadata. Inhomogeneities found in the Swedish and Finnish series were adjusted without metadata. Results further showed benefits of incorporating metadata to the automatically detected inhomogeneities. The inhomogeneities caused annual changes in the precipitation in the range of 0.72 to 1.46. Analysis of the inhomogeneities showed that relocations caused the highest adjustment factors. 56 % of all the adjusted inhomogeneities had adjustment factors below 1, which led to a more pronounced increase in the trend of the homogenized series. The homogenized series showed increasing trends in the period 1961-2018 except in autumn where a decreasing trend was observed. The highest trend was observed in the winter series while the greatest variation in trend size before and after homogenization was observed in the annual series. The most noticeable changes before and after homogenization were seen in the southeastern region of Troms and Finnmark in Northern Norway, where the highest decrease in both annual and seasonal precipitation was observed. Nevertheless, results after homogenization showed better regional coherence in comparison to the non-homogenized series.

In general, homogenization greatly improved the quality of precipitation series by reducing the regional variability and improving both the temporal and spatial coherence of the dataset. The dataset was thus more reliable in explaining the large-scale climate variations and was used to calculate the new climate normals in Norway.

5 References

Alexandersson H. 1986. A homogeneity test applied to precipitation data. Journal of Climatology, Vol. 6, 661-675.

Alexandersson H. and Moberg A. 1997. Homogenization of Swedish temperature data. Part I. Homogeneity test for linear trends. Int J Climatol 17: 25−34.

Azorin-Molina C., Guijarro J.A., McVicar T.R., Vicente-Serrano S.M., Chen D., Jerez S. and Espírito-Santo F. 2016. Trends of daily peak wind gusts in Spain and Portugal, 1961-2014. Journal of Geophysical Research - Atmospheres, 121(3), 1059–1078. https://doi.org/10.1002/2015JD024485

Azorin-Molina C., Rehman S., Guijarro J.A., McVicar T.R., Minola L., Chen D. and Vicente-Serrano S.M. 2018. Recent trends in wind speed across Saudi Arabia, 1978–2013. International Journal of Climatology, 38- (Supplement 1), e966–e984. https://doi.org/10.1002/joc.5423

Azorin-Molina C., Guijarro J.A., McVicar T.R., Trewin B.C., Frost A.J. and Chen D. 2019. An approach to homogenize daily peak wind gusts: an application to the Australian series. International Journal of Climatology, 39(4), 2260– 2277.

Coll J., Domonkos P., Guijarro J., Curley M., Rustemeier E., Aguilar E., Walsh S. and Sweeney J. 2020. Application of homogenization methods for Ireland's monthly precipitation records: comparison of break detection results. International Journal of Climatology, 1–20. https://doi.org/10.1002/joc. 6575.

Domonkos P. 2015. Homogenization of precipitation time series with ACMANT. Theoretical Applied Climatology, 122, 303–314. https://doi.org/10.1007/s00704-014-1298-5

Domonkos P. and Coll J. 2017. Homogenization of temperature and precipitation time series with ACMANT3: method description and efficiency tests. International Journal of Climatology, 37, 1910–1921. https://doi.org/10.1002/joc.4822

Førland E.J. 1979. Precipitation and topography. DNMI klima report 2/79.

Førland E.J. and Aune B. 1985a. Comparison of Nordic methods for point precipitation correction. In Sevruk, B. (ed), Correction of Precipitation Measurements, Zürcher Geographische Schriften 23, 239-244.

Førland E.J. and Aune B. 1985b. Comparison of Nordic methods for point precipitation correction. DNMI klima report 40/85.

Guijarro J.A. 2008. Homogenization of a dense thermo-pluviometric monthly database in the Balearic Islands using the free contributed R package Climatol. WMO Fifth Seminar for Homogenization and Quality Control in Climatological Databases, Budapest, Hungary; WCDMP-No. 68, WMO-TD No. 1434.

Guijarro J.A. 2015. Homogenization of Spanish mean wind speed monthly series. In: Lakatos, M. et al. (Eds.) 8th Seminar for Homogenization and Quality Control in Climatological Databases and Third Conference on Spatial Interpolation Techniques in Climatology and Meteorology, 12–16 May 2014, WMO Climate Data and Monitoring WCDMP-No. 84. Budapest, pp. 98–106.

Guijarro J.A. 2018. Homogenization of climatic series with Climatol. Version 3.1.1. Guide.

Guijarro J.A. 2019. Climatol: climate tools (series homogenization and derived products). R package version 3.1.2 https://CRAN.R-project.org/package=climatol

Hanssen-Bauer I. and Førland E.J. 1998, Annual and seasonal precipitation variations in Norway 1896-1997, DNMI Report No. 27/98 KLIMA

Hanssen-Bauer I., Førland E.J. 1994. Homogenizing Long Norwegian Series. Journal of Climate, Vol. 7, No. 6, 1001-1013.

Kuya E.K., Gjelten H.M. and Tveito O.E. 2020. Homogenization of Norway's mean monthly temperature series. MET Report 3/2020.

Lindau R. and V. Venema, 2016. The uncertainty of break positions detected by homogenization algorithms in climate records. International Journal of Climatology, 36, no. 2, pp. 576–589. https://doi.org/10.1002/joc.4366

Luna M.L., Guijarro J.A. and López J.A. 2012. A monthly precipitation database for Spain (1851–2008): reconstruction, homogeneity and trends. Advances in Science and Research, 8(1), 1–4. https://doi.org/10.5194/asr-8-1-2012

Lundstad E. 2016. Homogenization of daily precipitation in Norway. MET Report 12/2016.

Mamara A., Argiriou A.A. and Anadranistakis M. 2013. Homogenization of mean monthly temperature time series of Greece. International Journal of Climatology, 33(12), 2649–2666. https://doi.org/10.1002/joc.3614

Menne, M.J. and Williams C.N. 2009. Homogenization of Temperature Series via Pairwise Comparisons. J. Climate, 22, 1700–1717, https://doi.org/10.1175/2008JCLI2263.1

Mestre O., Domonkos P., Picard F., Auer I., Robin S., Lebarbier E., Böhm R., Aguilar E., Guijarro J., Vertachnik G., Klancar M., Dubuisson B. and Stepanek P. 2013. HOMER: a homogenization software - methods and applications. Idojaras-Quarterly Journal of the Hungarian Meteorological Service. 117, 47-67.

Nordli P.Ø., Hanssen-Bauer I. and Førland E.J. 1996. Homogeneity analyses of temperature and precipitation series from Svalbard and Jan Mayen, DNMI KLIMA Report 16/96.

Nygård H.D. 2004. Nedbørmålingar frå Geonor T-200 samanlikna med manuelle målingar. MET Norway ObsReport 008.

Paulhus J.L.H. and Kohler M.A. 1952. Interpolation of missing precipitation records. Monthly Weather Review, 80(8), 129–133. https://doi.org/10. 1175/1520-0493(1952)080<0129:IOMPR>2.0.CO;2

Peterson T.C., Easterling D.R., Karl T.R., Groisman P., Nicholls N., Plummer N., Torok S., Auer I., Boehm R., Gullett D., Vincint L., Heino R., Tuomenvirta H., Mestre O., Szentimrey T., Salinger J., Førland E.J., Hanssen-Bauer I., Alexandersson H., Jones P.D. and Parker D. 1998. Homogeneity adjustments of in situ atmospheric climate data: a review. International Journal of Climatology, 18(13), 1493–1517. https://doi.org/10.1002/(SICI)1097-0088(19981115)18:13<1493::AID-JOC329>3.0.CO;2-T

Ponce-Cruz R., Diakite L., Monterroso-Rivas A., Ontiveros-Capurata R. and Crespo-Pichardo, G. 2019. Homogenization of Monthly Rainfall Data Series in Lerma-Toluca Watershed with Climatol.

Rustemeier E., Kapala A., Meyer-Christoffer A., Finger P., Schneider U., Venema V., Ziese M., Simmer C. and Becker A. 2017. AHOPS Europe - a gridded precipitation data set from European homogenized time series. In: 9th Seminar for Homogenization and Quality Control in Climatological Databases. Geneva: WMO, pp. 88–101, WCDMP-85.

Szentimrey T. 1999. Multiple Analysis of Series for homogenization (MASH). Proceedings of the second seminar for homogenization of surface climatological data, Budapest, Hungary, WMO, WCDMP-No. 41, 27–46.

Szentimrey T. 2014. Multiple Analysis of Series for Homogenization, MASHv3.03, Hungarian Meteorological Service, p. 64.

Tveito O.E., Aniskevica S., Cappelen J., Engström E., Gjelten H.M., Jensen C.D., Jokinen P., Kuya E.K., Lussana C., Mändla K., Mäkelä A., Pärg R., Zandersons V. and Wern L. 2020. ClimNorm-temperature data set for regional analysis. MET Report 04/2020.

Venema V., Mestre O., Aguilar E., Auer I., Guijarro J.A., Domonkos P., Vertacnik G., Szentimrey T., Stepanek P., Zahradnicek P., Viarre J., Müller-Westermeier G., Lakatos M., Williams C.N., Menne M., Lindau R., Rasol D., Rustemeier E., Kolokythas K., Marinova T., Andresen L., Acquaotta F., Fratianni S., Cheval S., Klancar M., Brunetti M., Gruber C., Duran M.P., Likso T., Esteban P. and Brandsma T. 2012. Benchmarking monthly homogenization algorithms. Clim. Past 8: 89–115.

Venema V., Trewin B., Wang X., Szentimrey T., Lakatos M., Aguilar E., Auer I., Guijarro J.A., Menne M. and Oria C. 2018. Guidance on the homogenization of climate station data. https://doi.org/10.31223/osf.io/8qzrf

Wang X.L. and Feng F. 2013. RHtests_dlyPrcp User Manual. Climate Research Division, ASTD, Ontario, Toronto, Environment Canada.

Wang X.L. and Feng F. 2014. RHtestsV4 User Manual. Climate Research Division, Atmospheric Science and Technology Directorate, Science and Technology Branch, Environment Canada. http://etccdi.pacificclimate.org/software.shtml

World Meteorological Organization (WMO) 2020. Guidelines on Homogenization. WMO-No. 1245, Geneva, Switzerland.

6 Appendix

6.1 Norwegian precipitation series

Table A1: Norwegian precipitation series analyzed in this study, including station number, name, merged series, latitude, longitude, altitude and data period. Series with data prior to 1961 are marked with start year 1961. When two series have data in the same period, the data from the most recent series of the two is chosen in the merged series.*

Number	Name	Merged	Name	Lat	Lon	Alt	Start	End
60	Linnes			61.5581	12.499	564	1968	2018
100	Plassen			61.1349	12.5039	333	1968	2018
290	Tågmyra	300	Vola i Trysil	61.4167	12.0333	585	1961*	1966
		290	Tågmyra	61.4159	12.0661	557	1966	2010
420	Heggeriset-Nordstrand			61.6848	11.9963	481	1968	2018
610	Gløtvola-Trøan	600	Gløtvola	61.8442	11.8502	696	1961*	1999
		610	Gløtvola-Trøan	61.8433	11.8408	690	1997	2018
700	Drevsjø			61.8872	12.048	672	1961*	2018
730	Valdalen	122610	Grövelsjön (SE)	62.0991	12.3153	815	1961	1969
		730	Valdalen	62.0758	12.1722	794	1968	2018
770	Ellefsplass			62.204	11.4525	713	1968	2018
810	Tufsingdal-Midtdal	800	Tufsingdal	62.2477	11.7617	670	1961*	1990
		810	Tufsingdal-Midtdal	62.2776	11.732	687	1991	2018
1080	Hvaler			59.0367	11.0444	17	1961*	2018
1230	Halden			59.1223	11.388	3	1961*	2018
1400	Brekke sluse			59.1477	11.5583	114	1961*	2018
1650	Strømfoss			59.3006	11.6599	113	1961*	2018
1950	Ørje			59.4829	11.6506	123	1961*	2018
2650	Aurskog II	2610	Bjørkelangen II	59.8898	11.5816	135	1962	2012
		2650	Aurskog II	59.9119	11.5801	128	2008	2018
3200	Baterød	3200	Baterød	59.3072	11.1338	31	1961*	2018
3780	Igsi i Hobøl			59.636	11.0468	144	1961*	2018
4740	Ukkestad			60.1742	11.051	187	1965	2018

4780	Gardermoen			60.2065	11.0802	202	1961*	2018
5350	Nord-Odal			60.3883	11.558	147	1961*	2018
6020	Flisa II	6040	Flisa	60.6173	12.017	184	1961*	1998
		6020	Flisa II	60.6141	12.0125	185	2004	2018
6440	Vermundsjøen	6460	Finnskog	60.6914	12.4003	295	1961*	1989
		6440	Vermundsjøen	60.6925	12.369	276	1989	2018
6620	Elverum-Fagertun	6650	Elverum	60.8920	11.5605	188	1961*	1962
		6640	Elverum II	60.9002	11.5727	190	1962	1967
		6630	Elverum-Vier	60.9095	11.5925	221	1967	1978
		6620	Elverum-Fagertun	60.9107	11.593	230	1978	2013
7900	Finstad	7920	Finstad-Nyhus	62.10.83	11.0355	525	2011	2018
		7910	Finstad-Nytrøa	62.1050	11.0408	505	1998	2011
		7900	Finstad	62.1047	11.0503	513	1961*	1998
7950	Rena flyplass	7010	Rena-Haugedalen	61.1603	11.4427	240	1961*	2013
		7950	Rena flyplass	61.1847	11.3747	255	2011	2018
8720	Atnsjøen			61.8902	10.1398	749	1961*	2018
9160	Folldal-Fredheim	9100	Folldal	62.1264	10.0467	709	1961*	2006
		9160	Folldal-Fredheim	62.1282	9.9947	694	2011	2018
9870	Blanktjernmoen i Kvikne			62.4342	10.428	700	1961*	2018
10300	Håsjøen-Solgløtt	900	Langen	62.4342	11.8517	685	1968	2002
		10300	Håsjøen-Solgløtt	62.4698	11.7752	650	1997	2018
10380	Røros lufthavn	10400	Røros	62.5742	11.3787	628	1961*	2003
		10380	Røros lufthavn	62.5773	11.3518	625	2004	2018
10600	Aursund	10600	Aursund	62.6737	11.4534	685	1961*	2018
10800	Sølendet	10750	Brekkebygd	62.6420	11.8820	712	1961*	1986
		10740	Brekken	62.6452	11.8797	710	1986	2004
		10800	Sølendet	62.6793	11.8153	747	2007	2018
11120	Eidsvoll verk	11120	Eidsvoll verk	60.2987	11.16	181	1961*	2018
11710	Einavatn	11710	Einavatn	60.5952	10.6403	406	1968	2018
11900	Biri			60.9518	10.5954	190	1961*	2018
12200	Jønsberg landbruksskole			60.751	11.2065	218	1961*	2012
12520	Nes på Hedmark			60.7908	10.9583	205	1961*	2017
12600	Vea			60.953	10.679	161	1967	2018
12800	Mesna-Tyria	12750	Mesna	61.1167	10.6000	520	1961*	1962
		12800	Mesna-Tyria	61.1137	10.6707	520	1961	2015
13100	Vestre Gausdal			61.3453	9.7689	580	1961*	2008
13310	Søre Brekkom	13300	Sprangrudlien i Ringebu	61.4623	10.3053	755	1961*	1975
		13310	Søre Brekkom	61.4628	10.3097	770	1975	2018
13640	Olstappen			61.5145	9.4043	630	1970	2018
13700	Espedalen			61.4177	9.5408	752	1961*	2018

14050	Sjoa	14310	Otta-Bredvangen	61.7278	9.5443	285	1970	1995
		14050	Sjoa	61.6757	9.5562	330	1986	2018
14550	Preststulen			61.9225	9.1984	823	1961*	2018
14711	Grov-Solhaug	14710	Grov	61.8123	9.0152	808	1961*	1999
		14711	Grov-Solhaug	61.8135	9.0133	811	1999	2018
15430	Bøverdal	15430	Bøverdal	61.7207	8.2443	701	1961*	2018
15480	Skjåk II			61.8777	8.4672	374	1961*	2018
15660	Skjåk			61.9013	8.1706	432	1961*	2018
16610	Fokstugu	16600	Fokstua	62.1188	9.277	952	1961*	1968
		16610	Fokstugu	62.1133	9.2862	973	1968	2018
17150	Rygge			59.3742	10.798	40	1961*	2018
17251	Moss brannstasjon	17250	Moss	59.434	10.6667	31	1961*	2004
		17251	Moss brannstasjon	59.4425	10.6835	32	2004	2018
17500	Fløter			59.4963	11.0133	131	1971	2018
17741	Drøbak-Dyrløkke	17750	Drøbak	59.6762	10.6298	85	1961*	1976
		17740	Drøbak-Ullerud	59.6675	10.6452	76	1977	1991
		17741	Drøbak-Dyrløkke	59.6735	10.654	89	1991	2009
17850	Ås			59.6605	10.7818	92	1961*	2018
18160	Nordstrand			59.873	10.7912	118	1961*	2018
18450	Maridalsoset			59.9719	10.7894	173	1961*	2018
18500	Bjørnholt			60.0513	10.6878	360	1961*	2018
18700	Oslo-Blindern			59.9423	10.72	94	1961*	2018
19100	Kjelsås i Sørkedalen			60.0371	10.5963	319	1961*	2009
19610	Horni	19600	Stovi	59.9117	10.4581	117	1961*	1990
		19610	Horni	59.9153	10.4603	81	1998	2016
19710	Asker	19710	Asker	59.8558	10.4358	163	1961*	1977
		19720	Asker brannstasjon	59.8335	10.4358	112	1979	1982
		19710	Asker	59.8558	10.4358	163	1983	2018
20250	Hole			60.1088	10.2948	66	1961*	2018
20520	Lunner			60.295	10.5753	372	1961*	2018
21360	Odnes			60.8008	10.1173	156	1961*	2009
22730	Hedal i Valdres II	22720	Hedal i Valdres	60.6217	9.7178	503	1961*	1968
		22730	Hedal i Valdres II	60.6197	9.7238	474	1968	2018
22840	Reinli			60.8346	9.4905	628	1961*	2018
23160	Åbjørsbråten			60.918	9.2893	639	1961*	2017
23390	Lykkja i Hemsedal	23400	Lykkja i Hemsedal	60.883	8.8333	861	1961*	1992
		23390	Lykkja i Hemsedal	60.8837	8.8293	890	1993	2008
23560	Beito			61.2433	8.8557	754	1961*	2018
23720	Vang i Valdres			61.124	8.569	489	1961*	2018
24210	Sokna II			60.238	9.9267	140	1961*	2018

24600	Grimeli i Krødsherad			60.137	9.5958	367	1961*	2018
24710	Gulsvik II	24770	Gulsvik IV	60.3897	9.573	149	1961*	2009
		24710	Gulsvik II	60.383	9.605	142	2007	2018
24960	Gol-Stake			60.7188	8.9478	542	1964	2018
25100	Hemsedal-Hølto	25080	Hemsedal	60.857	8.6033	608	1961*	1981
		25100	Hemsedal-Hølto	60.8703	8.5285	648	1982	2018
25260	Vats-Randen	25240	Vats	60.6842	8.3044	800	1961*	2000
		25260	Vats-Randen	60.6785	8.2783	863	2001	2017
25320	Ål III			60.6391	8.5609	720	1961*	2018
25640	Geilo			60.532	8.1483	841	1961*	2018
26161	Modum-S.Kopland	26160	Fossum i Modum	59.9125	9.8755	116	1961*	2001
		26161	Modum-S.Kopland	59.9172	9.8605	80	2003	2010
26240	Hiåsen			60.0122	9.51	402	1961*	2013
26380	Eggedal III	26400	Eggedal	60.2617	9.2812	463	1961*	1966
		26370	Eggedal II	60.2437	9.3522	271	1966	1981
		26380	Eggedal III	60.2475	9.3443	293	1981	2017
26670	Hakavik			59.6252	9.9534	21	1964	2018
27301	Ramnes-Berg	27300	Ramnes	59.3562	10.2501	44	1961*	2003
		27301	Ramnes-Berg	59.3562	10.2501	30	2003	2018
27600	Sandefjord			59.132	10.2147	6	1961*	2018
27800	Hedrum			59.196	9.9641	31	1961*	2018
28380	Kongsberg brannstasjon	28360	Kongsberg II/III	59.6633	9.6483	171	1961*	1979
		28370	Kongsberg IV	59.663	9.65	168	1979	2002
		28380	Kongsberg brannstasjon	59.6247	9.6377	170	2003	2018
28922	Veggli II	28921	Veggli-S.Bjørkgård	60.0427	9.1683	220	2003	2009
		28920	Veggli	60.0518	9.1542	243	1961*	2003
		28922	Veggli II	60.0435	9.1468	275	2006	2018
29350	Uvdal kraftverk	29310	Uvdal II	60.2682	8.7798	486	1961*	2008
		29350	Uvdal kraftverk	60.255	8.7057	648	1985	2018
29600	Tunhovd			60.4629	8.7511	870	1961*	2018
30320	Skien-Elstrøm	30290	Skien II	59.2078	9.6064	24	1968	1987
		30320	Skien-Elstrøm	59.1992	9.5895	13	1985	2018
30380	Godal	30370	Besstul i Gjerpen	59.447	9.5385	460	1961*	2002
		30380	Godal	59.4558	9.5337	475	2002	2018
30530	Notodden			59.5688	9.2643	34	1961*	2018
30860	Bergeligrend			59.8861	9.058	514	1961*	2018
31080	Tessungdalen-Bakkhus	31100	Tessungdalen	60.1283	8.6703	775	1961*	1982
		31080	Tessungdalen-Bakkhus	60.1293	8.7033	762	1983	2018
31410	Rjukan			59.88	8.6663	258	1961*	2018
31570	Møsvatn-Haug	31610	Møsstrand	59.8522	8.0648	948	1967	1976

		31570	Møsvatn-Haug	59.815	8.1363	946	1976	2018
31660	Mogen			60.018	7.913	954	1961*	2018
31900	Tuddal			59.7463	8.8083	464	1961*	2018
32200	Lifjell			59.455	9.0372	354	1961*	2011
32350	Åmotsdal			59.6478	8.3768	567	1971	2018
32780	Høidalen i Solum			59.1444	9.2668	113	1961*	2018
32850	Kviteseid-Moen			59.4058	8.473	77	1971	2018
32890	Høydalsmo II	32900	Høydalsmo	59.4977	8.2012	573	1961*	2004
		32890	Høydalsmo II	59.497	8.1992	560	2006	2018
33250	Rauland			59.7057	8.0317	715	1961*	2018
34580	Drangedal-Refdalskilen	34600	Drangedal	59.0993	9.0677	82	1961*	20018
		34620	Drangedal II	59.1075	9.0475	106	2009	2016
		34580	Drangedal-Refdalskilen	59.0767	9.0687	65	2017	2018
34800	Tørdal-Suvdøla	34790	Tørdal II	59.1482	8.794	162	1961*	1995
		34800	Tørdal-Suvdøla	59.1482	8.7742	235	1996	2018
34900	Postmyr i Drangedal			59.2647	8.7686	464	1961*	2018
35090	Eikeland	35080	Egelands verk	58.8	9.1167	46	1961*	1979
		35090	Eikeland	58.8037	9.098	42	1980	2018
35340	Risør brannstasjon	35350	Risør	58.7167	9.234	20	1961*	1967
		35340	Risør brannstasjon	58.7182	9.2103	36	1968	2018
36110	Arendal brannstasjon II	36100	Østre Moland	58.4817	8.7555	40	1961*	1973
		36060	Arendal brannstasjon	58.468	8.7595	44	1967	2013
		36110	Arendal brannstasjon II	58.4613	8.7228	50	2013	2018
36200	Torungen fyr			58.3988	8.7893	12	1961*	2018
36560	Nelaug	36580	Nelaug-Øynes	58.6705	8.617	147	1961*	1966
		36560	Nelaug	58.6582	8.63	142	1966	2018
37230	Tveitsund			59.0257	8.5187	252	1961*	2018
37500	Foldsæ			59.3242	8.1517	532	1961*	2018
37650	Kilegrend			59.0095	8.2735	287	1961*	2018
37740	Fyresdal-Ålandsli	37750	Fyresdal	59.169	8.038	303	1961*	2006
		37740	Fyresdal-Ålandsli	59.162	8.0398	295	2007	2018
38140	Landvik			58.34	8.5225	6	1961*	2018
38380	Dovland			58.5234	8.0392	259	1961*	2018
38421	Senumstad	38420	Rislå	58.4248	8.3002	66	1961*	1999
		38421	Senumstad	58.4213	8.2893	67	1999	2018
38450	Herefoss			58.5222	8.35	85	1961*	2014
38600	Mykland			58.633	8.2888	245	1961*	2018
38800	Tovdal			58.7938	8.2295	220	1961*	2018
39040	Kjevik			58.2	8.0767	12	1961*	2018
39220	Mestad i Oddernes			58.2153	7.89	151	1961*	2018

39750	Byglandsfjord-Neset	39710	Byglandsfjord II	58.6655	7.8117	206	1961*	1969
		39690	Byglandsfjord-Solbakken	58.6662	7.8085	212	1970	2011
		39750	Byglandsfjord-Neset	58.6863	7.803	207	2011	2018
40420	Bykle-Kultran	40400	Bykle	59.3504	7.3347	613	1961*	1967
		40420	Bykle-Kultran	59.3515	7.3445	599	1967	2018
41090	Mandal III	41110	Mandal II	58.0475	7.4472	138	1961*	2007
		41090	Mandal III	58.0247	7.4517	10	2009	2018
41200	Finsland	41350	Bjelland	58.35	7.5333	80	1961*	1972
		41200	Finsland	58.3195	7.5927	275	1971	2018
41480	Åseral			58.6172	7.4128	268	1961*	2018
41550	Ljosland-Monen	41560	Ljosland	58.7908	7.3508	547	1961*	1971
		41550	Ljosland-Monen	58.7878	7.3501	504	1971	2018
41640	Vigmostad			58.2221	7.3363	38	1961*	2010
41770	Lindesnes fyr	41760	Lindesnes fyr	57.9828	7.0467	17	1961*	1969
		41770	Lindesnes fyr	57.9826	7.0478	16	1969	2018
41860	Kvineshei-Sørhelle	41880	Kvinesdal	58.3	7.05	343	1961*	1985
		41860	Kvineshei-Sørhelle	58.2435	6.9827	317	1986	2018
42160	Lista fyr			58.109	6.5675	14	1961*	2018
42250	Fedafjorden II			58.281	6.816	26	1961*	2018
42520	Risnes i Fjotland			58.6577	6.9443	348	1961*	2018
42650	Drangeid			58.2842	6.6498	5	1961*	2018
42720	Bakke			58.4117	6.657	75	1961*	2018
42950	Øvre Sirdal			58.9455	6.9183	582	1961*	2018
43360	Egersund			58.4527	6.003	4	1961*	2018
43810	Maudal			58.7645	6.3675	311	1961*	2018
44160	Hognestad			58.6947	5.6418	19	1961*	2018
44480	Søyland i Gjesdal			58.6855	5.9817	263	1961*	2018
44520	Helland i gjesdal			58.755	6.0135	288	1962	2018
44560	Sola			58.8843	5.637	7	1961*	2018
44800	Sviland			58.8185	5.9202	230	1961*	2018
44900	Oltedal	44880	Høgsfjord	58.8347	6.0933	65	1961*	1961
		44890	Høgsfjord II	58.834	6.0878	52	1961	1972
		44900	Oltedal	58.8286	6.0553	44	1972	2018
45350	Lysebotn			59.0552	6.6467	5	1961*	2018
45600	Bjørheim i Ryfylke			59.0743	6.019	64	1961*	2018
46150	Sand i Ryfylke II			59.4791	6.276	25	1961*	2018
46300	Suldalsvatn			59.5887	6.809	333	1961*	2018
46450	Røldal			59.8304	6.8238	393	1961*	2018
46610	Sauda			59.6478	6.35	5	1961*	2018
46850	Hundseid i Vikerdal			59.5532	5.9902	159	1961*	2018

46930	Vats i Vindafjord	46910	Nedre Vats	59.484	5.7507	64	1969	2012
		46930	Vats i Vindafjord	59.4927	5.7208	20	2011	2018
47090	Skjold-Frøvik	47120	Skjold-Viken	59.5	5.6	11	1961*	1986
		47090	Skjold-Frøvik	59.5033	5.6257	5	1986	2018
47300	Utsira fyr			59.3065	4.8723	55	1961*	2018
47498	Etne II	47500	Etne	59.6648	5.9655	35	1961*	2015
		47498	Etne II	59.6625	5.9538	8	2015	2018
47600	Litledal			59.6642	6.0657	83	1961*	2018
47750	Vintertun	49250	Jøsendal	59.9314	6.5787	345	1961*	1973
		47750	Vintertun	59.9102	6.5098	395	1973	2008
47820	Eikemo			59.8594	6.2786	178	1961	2018
47890	Opstveit	47900	Indre Matre	59.8591	5.9909	24	1961*	1971
		47890	Opstveit	59.8547	6.0167	38	1968	2018
48250	Fitjar-Prestbø	48260	Fitjar	59.9167	5.3167	20	1961*	1982
		48250	Fitjar-Prestbø	59.9167	5.3163	24	1982	2010
48450	Husnes			59.8643	5.7698	13	1966	2018
48500	Rosendal			59.9913	6.0263	75	1961*	2018
49080	Øvre Krossdalen	49050	Jondal i Hordaland	60.2818	6.3032	95	1961*	1966
		49070	Kvåle	60.2803	6.3778	342	1966	2012
		49080	Øvre Krossdalen	60.2795	6.3857	342	2013	2018
49351	Tyssedal Ia	49350	Tyssedal I	60.1198	6.5608	32	1961*	2001
		49351	Tyssedal Ia	60.1188	6.5547	4	2000	2018
49550	Kinsarvik			60.3725	6.7382	108	1961*	2008
49631	Eidfjord II	49630	Eidfjord	60.4668	7.0723	5	1961*	2002
		49631	Eidfjord II	60.4647	7.0692	20	2003	2018
49800	Fet i Eidfjord	49850	Maurset	60.4167	7.3333	778	1970	1973
		49750	Liset	60.4226	7.2739	748	1974	2010
		49800	Fet i Eidfjord	60.4085	7.2798	735	1961*	1970
		49800	Fet i Eidfjord	60.4085	7.2798	735	2006	2018
50080	Øystese-Borge	50100	Øystese	60.3667	6.2	20	1961*	1961
		55090	Øystese-Mo	60.3853	6.1845	68	1961	1980
		50080	Øystese-Borge	60.379	6.1927	108	1980	2018
50150	Hatlestrand			60.045	5.9032	45	1961*	2018
50450	Fana-Stend			60.2728	5.3305	54	1961*	2018
51250	Øvstedal			60.6887	5.9647	316	1961*	2018
51470	Bulken			60.6455	6.222	328	1961*	2018
51530	Vossevangen	51560	Voss II	60.6275	6.4253	61	1961*	1961
		51580	Voss-Tvilde	60.6383	6.4516	121	1962	1967
		51590	Voss-Bø	60.6421	6.4893	125	1967	2003
		51530	Vossevangen	60.625	6.4262	54	2004	2018

52170	Eksingedal			60.8028	6.1469	450	1961*	2018
52220	Gullbrå			60.8288	6.2645	579	1961*	2018
52310	Modalen III	52300	Modalen	60.8383	5.9333	104	1961*	1980
		52290	Modalen II	60.841	5.9533	114	1980	2008
		52310	Modalen III	60.8562	5.9733	125	2008	2018
52400	Eikanger-Myr			60.6268	5.3742	72	1968	2018
52601	Haukeland-Storevatn	52600	Haukeland	60.8248	5.5732	196	1961*	2002
		52601	Haukeland-Storevatn	60.8347	5.5833	325	2003	2017
52750	Frøyset			60.8462	5.2108	13	1961*	2018
52860	Takle			61.0272	5.3813	38	1961*	2018
52930	Brekke i Sogn			60.9585	5.425	240	1961*	2018
53070	Vik i Sogn III			61.0728	6.5813	65	1963	2018
53101	Vangsnes	53100	Vangsnes	61.1722	6.6435	51	1961*	1994
		53101	Vangsnes	61.1724	6.6452	49	1993	2018
53700	Aurland			60.9027	7.201	15	1961*	2018
54500	Borlo			61.0742	7.9553	502	1961*	2008
54600	Maristova			61.1093	8.036	806	1961*	2018
55550	Hafslo			61.2925	7.1887	246	1961*	2018
55730	Sogndal-Selseng			61.3348	6.9335	421	1961*	2018
55820	Fjærland-Bremuseet	55840	Fjærland-Skarestad	61.4352	6.7707	10	1961*	2005
		55820	Fjærland-Bremuseet	61.4233	6.7642	3	2005	2018
56010	Høyanger verk	56120	Høyangshåland	61.2315	6.083	243	1961*	1992
		56010	Høyanger verk	61.22	6.0702	15	1981	2018
56280	Rørvikvatn			61.2163	5.7513	350	1961*	2013
56320	Lavik			61.1122	5.5413	31	1961*	2018
56400	Ytre Solund			61.007	4.6693	3	1961*	2018
56520	Hovlandsdal			61.232	5.4342	85	1961*	2018
56780	Sygna	56800	Gaular	61.328	5.798	79	1961*	1995
		56780	Sygna	61.3435	5.7267	47	1996	2018
56960	Haukedal			61.4202	6.3758	311	1961*	2018
57390	Skei i Jølster			61.5722	6.4873	205	1969	2018
57480	Botnen i Førde			61.5349	6.0586	237	1961*	2018
57660	Eimhjellen	57640	Solheim i Gloppen	61.6315	5.7198	177	1961*	1991
		57660	Eimhjellen	61.6415	5.8163	170	1981	2018
57680	Eikefjord			61.5888	5.472	30	1961*	2007
57810	Svelgen II	57800	Svelgen	61.7683	5.2967	16	1961*	1972
		57810	Svelgen II	61.7707	5.2983	16	1973	2018
57850	Daviknes	57870	Davik	61.8892	5.5547	32	1961*	1970
		57860	Davik II	61.8833	5.55	3	1970	1990
		57850	Daviknes	61.8986	5.5333	78	1990	2018

57940	Ålfoten II			61.832	5.6674	24	1961*	2018
58070	Sandane			61.788	6.1837	51	1961*	2018
58320	Myklebust i Breim			61.708	6.6092	315	1961*	2018
58390	Innvik-Heggedal	58400	Innvik	61.8501	6.6256	32	1961*	2005
		58390	Innvik-Heggedal	61.838	6.6	70	2005	2018
58480	Oldedalen			61.694	6.8088	44	1961*	2018
58960	Hornindal			62.0033	6.6497	349	1961*	2018
59250	Refvik	59200	Ulvesund	61.9663	5.1383	1	1961*	1996
		59250	Refvik	61.9985	5.088	3	1996	2018
59450	Stadlandet			62.1467	5.2115	75	1961*	2018
59610	Fiskåbygd			62.103	5.5817	41	1969	2018
59670	Ekset i Volda			62.1671	6.037	58	1961*	2008
60400	Norddal			62.2477	7.2392	28	1961*	2018
60500	Tafjord			62.2305	7.4218	11	1961*	2018
60800	Ørskog			62.4775	6.8167	5	1961*	2018
60890	Brusdalsvatn II	60900	Brusdalsvann	62.4663	6.4639	188	1961*	1972
		60890	Brusdalsvatn II	62.4654	6.4013	33	1972	2018
60945	Ålesund IV	60970	Ålesund III	62.4762	6.2015	136	1961*	2004
		60945	Ålesund IV	62.4703	6.2108	15	2009	2018
60990	Vigra			62.5617	6.115	22	1961*	2018
61350	Åndalsnes			62.5658	7.6773	20	1961*	2018
61550	Verma			62.3418	8.0517	247	1961*	2009
61770	Leasjaskog			62.2317	8.3733	621	1961*	2008
61820	Eresfjord			62.663	8.105	14	1961*	2018
62700	Hustadvatn			62.9087	7.2436	80	1961*	2018
62900	Eide på Nordmøre			62.8915	7.3905	49	1961*	2018
63100	Øksendal			62.6855	8.4219	47	1961*	2018
63420	Sunndalsøra III	63420	Sunndalsøra III	62.6752	8.5617	10	1961*	2018
63580	Ångårdsvatnet			62.6708	9.1967	596	1965	2018
63750	Mjøen			62.5738	9.646	512	1965	2018
64460	Halsafjord II			62.978	8.2393	12	1961*	2014
64580	Ålvundfjord			62.8347	8.5213	5	1961*	2013
64800	Surnadal			63.0043	9.0107	39	1961*	2009
64900	Rindal			63.038	9.2205	228	1961*	2017
65230	Hemne-Lenes	65220	Hemne	63.2588	9.0038	133	1961*	1998
		65230	Hemne-Lenes	63.2613	9.0115	45	1998	2018
65270	Søvatnet			63.2302	9.3488	306	1965	2018
65370	Smøla-Moldstad			63.4197	8.063	30	1963	2018
65451	Hitra-Sandstad II	65450	Sandstad	63.5212	9.0943	20	1961*	2008
		65451	Hitra-Sandstad II	63.5187	9.1125	13	2012	2018

65600	Hitra			63.6238	8.7208	23	1961*	2013
66070	Skjenaldfossen i Orkdal			63.2942	9.7292	84	1961*	2017
66100	Songli			63.3308	9.6488	300	1961*	2013
66620	Rennebu-Ramstad	66600	Rennebu	62.8667	9.8333	360	1961*	1990
		66620	Rennebu-Ramstad	62.864	9.8354	223	1992	2018
66850	Kvikne i Østerdal			62.5962	10.271	549	1961*	2018
67150	Leinstrand			63.3281	10.2733	13	1961*	2018
67540	Røsbjørgen			62.9975	10.5199	330	1961*	2010
68270	Løksmyr			63.2315	10.4369	173	1961*	2018
68330	Lien i Selbu			63.2088	11.1132	255	1961*	2010
68420	Aunet			63.0556	11.5669	302	1961*	2018
68840	Stugudal-Kåsen	68800	Stugudal	62.8992	11.8744	614	1961*	1978
		68840	Stugudal-Kåsen	62.8952	11.8626	730	1978	2018
69100	Værnes			63.4597	10.9305	12	1961*	2018
69230	Hegra II			63.4402	11.2563	33	1961*	2010
69380	Meråker-Vardetun	69360	Meråker II	63.4229	11.7604	218	1961	1969
		69340	Meråker - Lillesve	63.4382	11.6915	115	1969	1973
		69330	Meråker - Krogstad	63.4431	11.6992	145	1974	1993
		69370	Meråker - Utsyn	63.4188	11.7588	239	1994	2004
		69380	Meråker-Vardetun	63.4115	11.7277	169	2004	2018
69420	Kluksdal	69410	Rotvoll	63.2727	11.806	587	1962	1998
		69420	Kluksdal	63.2855	11.9045	521	2000	2018
69550	Østås i Hegra			63.4871	11.3536	174	1961*	2018
69960	Buran			63.7199	11.5436	182	1962	2018
70480	Skjækerfossen			63.839	12.0217	110	1961*	2010
70510	Vera II	70500	Vera	63.8007	12.3873	368	1966	2012
		70510	Vera II	63.7853	12.3815	377	2013	2018
70820	Utgård II			64.1163	11.729	50	1962	2018
70850	Snåsa-Kjevlia			64.1587	12.4692	195	1961*	2018
71280	Leksvik-Myran	71270	Leksvik	63.6811	10.6025	139	1961*	1970
		71280	Leksvik-Myran	63.6856	10.6075	138	1970	2018
71550	Ørland III			63.7045	9.6105	10	1961*	2018
71750	Breivoll			63.918	10.4055	94	1966	2018
71810	Åfjord-Momyr	71800	Måmyr i Åfjord	64.0863	10.4942	250	1961*	1974
		71810	Åfjord-Momyr	64.1003	10.523	280	1975	2018
71900	Bessaker			64.2448	10.3257	12	1961*	2018
72100	Namdalseid			64.2508	11.2002	86	1961*	2011
72250	Bangdalen			64.3317	11.5438	62	1961*	2014
72650	Overhalla-Unnset	72700	Overhalla	64.4871	11.919	27	1961*	1977
		72650	Overhalla-Unnset	64.4815	11.8397	26	1977	2018

73250	Sørli			64.2432	13.765	370	1961*	2018
73800	Tunnsjø			64.6837	13.6506	376	1961*	2018
74350	Namsskogan	74300	Kjelmoen	64.716	12.7922	116	1968	1991
		74320	Trones-Tromsstad	64.7288	12.8155	143	1992	2018
		74350	Namsskogan	64.7422	12.846	140	1961*	1968
		74350	Namsskogan	64.7422	12.846	140	2006	2018
74530	Namsskogan-Bergli	74500	Øvre Namsskogan	64.9263	13.1562	214	1961*	1966
		74510	Sandåmo	64.9205	13.1817	216	1966	1999
		74530	Namsskogan-Bergli	64.9463	13.194	285	1999	2011
75100	Liafoss			64.8382	11.9547	44	1961*	2018
76100	Øksingøy			65.1245	12.3745	24	1961*	2018
77850	Susendal			65.3675	14.2457	498	1961*	2018
78180	Drevvassbygda	78100	Drevja	65.9925	13.3855	63	1961*	2001
		78180	Drevvassbygda	66.0713	13.4353	100	1998	2011
78250	Leirfjord			66.0668	12.9097	53	1961*	2018
78370	Bjerka-Valla	78410	Korgen II	66.0833	13.8333	10	1961*	1979
		78420	Korgen-Auringmoen	66.0932	13.8138	50	1979	1993
		78370	Bjerka-Valla	66.1415	13.8067	20	1994	2018
78610	Tustervatnet II			65.8302	13.9067	439	1961*	2017
78770	Famvatnet			65.7965	14.4873	510	1968	2016
78850	Røssvatn-Heggmo			65.9103	14.2722	399	1961*	2008
79480	Mo i Rana III			66.307	14.1542	41	1961*	2018
80200	Lurøy			66.3892	13.1848	115	1961*	2018
80610	Myken	80600	Myken	66.7605	12.4775	19	1961*	1991
		80610	Myken	66.7628	12.486	17	1992	2018
80850	Sundsfjord	80850	Sundsfjord	66.9712	14.1543	11	1962	1985
		80850	Sundsfjord	66.9712	14.1543	11	1989	2012
		80840	Sundsfjord-Tverrlia	66.9667	14.1333	70	1985	1988
81730	Junkerdal	81750	Graddis fjellstue	66.7423	15.739	429	1961*	1978
		81730	Junkerdal	66.8012	15.5787	210	1977	2011
81900	Sulitjelma			67.1348	16.0712	142	1961*	2018
82290	Bodø VI			67.267	14.3637	11	1961*	2018
82840	Styrkesnes-Hestvika	82850	Sørfold	67.5343	15.4726	21	1961*	1978
		82860	Styrkesnes	67.5333	15.4667	54	1978	1990
		82840	Styrkesnes-Hestvika	67.5258	15.4953	27	1991	2018
83300	Steigen			67.923	15.1123	31	1961*	2018
84070	Bjørkåsen	84100	Hestnes i Ballangen II	68.3085	16.7878	104	1961*	1964
		84070	Bjørkåsen	68.3302	16.7883	53	1964	2018
84190	Skjomen-Stiberg	84200	Skjomen	68.1821	17.5535	56	1961*	1987
		84190	Skjomen-Stiberg	68.2075	17.5145	29	1987	2019

85540	Leknes i Lofoten			68.1417	13.6057	13	1961*	2018
85660	Reine	85780	Glåpen fyr	67.8833	13.05	31	1961*	1984
		85660	Reine	67.9263	13.0865	17	1968	2017
86740	Bø i Vesterålen III	86760	Bø i Vesterålen II	68.6322	14.463	12	1961	2001
		86740	Bø i Vesterålen III	68.6067	14.4333	8	2002	2018
86850	Barkestad			68.8174	14.8003	3	1961*	2010
86950	Alsvåg i Vesterålen II			68.9147	15.2107	18	1961*	2018
87110	Andøya	87100	Andenes	69.3237	16.1199	5	1961*	1972
		87110	Andøya	69.3073	16.1312	10	1964	2018
87750	Gausvik			68.609	16.4947	7	1961*	2018
88100	Bones i Bardu			68.6457	18.2442	230	1961*	2018
89350	Bardufoss			69.0577	18.5437	76	1961*	2018
89500	Sætermoen II			68.8607	18.3373	114	1961*	2017
89650	Innset i Bardu			68.6577	18.8193	314	1961*	2017
89940	Dividalen II	89950	Dividalen	68.7783	19.71	228	1961*	2009
		89940	Dividalen II	68.7817	19.7017	204	2009	2018
90200	Storsteinnes i Balsfjord			69.2466	19.2274	27	1961*	2010
90450	Tromsø			69.6536	18.9368	100	1961*	2018
90490	Tromsø-Langnes			69.6767	18.9133	8	1964	2018
92350	Nordstraum i Kvænangen			69.8362	21.8958	20	1965	2018
93140	Alta lufthavn	93150	Alta aeradio	69.9715	23.3587	62	1961*	1963
		93140	Alta lufthavn	69.9775	23.3582	3	1963	2018
93301	Suolovuopmi-Lulit	93300	Suolovuopmi	69.5883	23.5317	377	1961*	2004
		93301	Suolovuopmi-Lulit	69.5797	23.5345	381	2004	2018
93500	Jotkajavre			69.7545	23.9342	389	1961*	2007
93900	Sihccajavri			68.7553	23.5387	382	1961*	2018
94130	Porsa II			70.3992	23.6257	38	1961*	2018
94170	Skaidi II			70.4415	24.4662	90	1961*	2018
95350	Banak	95400	Lakselv	70.0512	25.0087	7	1961*	1966
		95350	Banak	70.06	24.99	5	1965	2018
95590	Børselv II	95600	Børselv	70.3172	25.5472	10	1961*	1984
		95610	Børselv-Høgbakken	70.3207	25.547	13	1984	2015
		95590	Børselv II	70.3128	25.5642	23	2015	2018
96220	Lebesby-Karlmyhr	96210	Lebesby II	70.5732	27.0022	8	1961*	1980
		96220	Lebesby-Karlmyhr	70.5815	26.9938	18	1981	2018
96800	Rustefjelbma			70.3968	28.1928	10	1961*	2013
96931	Polmak Tollsted	96920	Polmak	70.0785	27.9865	21	1961*	1968
		96910	Polmak II	70.0692	28.0112	21	1968	1980
		96930	Polmak	70.0812	27.9792	30	1980	1998
		96931	Polmak Tollsted	70.0733	28.0012	18	1999	2018

97251	Karasjok-Markannjarga	97250	Karasjok	69.4683	25.4817	155	1961*	2012
		97251	Karasjok-Markannjarga	69.4635	25.5023	131	2004	2018
97350	Cuovddatmohkki			69.3695	24.4312	286	1961*	2018
98550	Vardø radio			70.3707	31.0962	10	1961*	2018
99330	Veines i Neiden			69.7038	29.2523	44	1961*	2012

6.2 Swedish and Finnish precipitation series

Table A2: Swedish and Finnish precipitation series used in the analysis, including station number, name, latitude, longitude, altitude and station number for series used for merging. SE and FI indicate Swedish and Finnish stations respectively.

	Number	Name	Lat	Lon	Alt	Merged
SE	81540	Nordkoster A	58.8952	11.004	10	81640
SE	81570	Håvelund	58.9453	11.4385	99	
SE	82490	Bäckefors	58.8055	12.1581	150	
SE	92120	Svaneholm D	59.1745	12.5484	95	92110
SE	92130	Blomskog A	59.2218	12.0781	170	91130, 92600
SE	92290	Sölje D	59.4846	12.6959	70	92260
SE	92410	Arvika A	59.6748	12.6383	66	92400, 92430
SE	92530	Charlottenberg	59.8837	12.2932	135	
SE	102400	Kindsjön D	60.6581	12.7119	415	
SE	102440	Letafors D	60.7389	12.698	335	
SE	102460	Tåsan	60.7677	12.8455	260	
SE	102470	Järpliden	60.7798	12.4593	430	
SE	102540	Höljes	60.9066	12.5843	230	
SE	103210	Vitsand D	60.3252	13.0065	150	102240
SE	103260	Stöllet D	60.4313	13.2446	145	103240
SE	112020	Löten D	61.0255	12.8399	425	
SE	112170	Grundforsen	61.2797	12.8568	412	
SE	112520	Idre D	61.8592	12.719	450	
SE	114140	Älvdalen A	61.2536	14.0355	252	114160, 114150
SE	114360	Ulvsjö	61.6022	14.1847	600	114330
SE	122330	Ljusnedal	62.5493	12.6043	585	
SE	122370	Malmagen	62.6094	12.1605	785	
SE	132170	Storlien-Storvallen A	63.2826	12.1218	583	132180, 132620
SE	132310	Häggsjön	63.5158	12.7159	480	132360
SE	132450	Sandnäset	63.7542	12.4291	432	
SE	132590	Edevik	63.9812	12.8709	425	142030
SE	133100	Vallbo	63.15	13.08	575	
SE	133190	Mörsil	63.3193	13.6488	400	

SE	133240	Järpströmmen	63.3915	13.388	380	
SE	133420	Olden D	63.6951	13.6473	344	133400
SE	143440	Jormlien	64.7307	13.9694	360	
SE	144040	Valsjöbyn	64.67	14.13	370	
SE	144310	Gäddede A	64.5044	14.2207	553	144300
SE	144560	Leipikvattnet	64.9290	14.1563	481	
SE	145500	Avasjö-Borgafjäll D	64.8366	15.0918	530	
SE	155730	Ransaren D	65.1391	15.0472	560	
SE	155900	Boksjö	65.6772	15.8245	475	
SE	155940	Hemavan-Mosekälla	65.8139	15.1139	550	155930
SE	166810	Jäckvik	66.3824	16.9959	430	
SE	180750	Malmberget	67.1705	20.6686	393	180730
SE	183920	Parkajoki	67.7314	23.486	200	
SE	188800	Abisko	68.3557	18.8206	388	
SE	188820	Katterjåkk	68.4219	18.1699	500	188830
SE	191910	Naimakka A	68.6762	21.5229	402	191900
FI	102035	Utsjoki Kevo	69.756	27.007	107	

6.3 Accepted breaks in the Norwegian series

Table A3. Date, SNHT-value, adjustment factor (AF) and metadata for accepted breaks in the Norwegain precipitation series.

Number	Name	Date	SNHT	AF	Metadata
730	Valdalen	01.07.1968	30.9	1.21	Relocation. Merged series 46122600 and 730.
1650	Strømfoss sluse	01.10.1986	56.7	0.92	New equipment 22.05.1985. New observer 1984 and 1993.
2650	Aurskog II	01.10.2007	23.3	0.89	Automation.
4780	Gardermoen	01.10.1972	60.1	0.89	Relocation 190 m ENE
10300	Håsjøen-Solgløtt	01.09.1997	25.8	0.81	Relocation 6 km NW. Merged series 900 and 10300.
10600	Aursund	01.09.1996	23.9	0.89	New equipment in September 1998. Possible environmental change - unkempt vegetation growing around gauge.
12800	Mesna-Tyria	01.03.1985	23.1	0.90	New observer
13100	Vestre Gausdal	01.12.1985	22.1	0.91	New observer
13640	Olstappen	01.06.2006	27.5	0.95	Automation and relocation.
13700	Espedalen	01.10.1992	31.6	1.05	Relocation 25-30 m NW.
17251	Moss brannstasjon	01.03.2004	22.2	0.99	Relocation 1.3 km NE. Merged series 17250 and 17251.
18450	Maridalsoset	01.11.1972	22.6	1.05	Relocation 70 m N and gauge equipped with windshield.
20520	Lunner	01.08.1982	27	0.91	New observer. Also cut down a few trees by the gauge prior to this.
22730	Hedal i Valdres II	01.01.2001	26.7	1.04	Relocation 150 m S.

23390	Lykkja i Hemsedal	01.01.1993	31.6	1.03	Relocation 200 m E. Merged series 23400 and 23390.
24710	Gulsvik II	01.12.2007	22.7	1.06	Automation and relocation. Merged series 24770 and 24710.
24960	Gol-Stake	01.10.1992	40.8	0.90	Relocation. And new observer, and new building close to gauge at about the same time.
25100	Hemsedal-Hølto	01.09.2000	29.1	1.13	Environmental change - removed some vegetation around gauge.
25260	Vats-Randen	01.09.2001	43	1.08	Relocation 1.6 km SW. Merged series 25240 and 25260.
27600	Sandefjord	01.06.1999	48.4	1.14	Relocation.
29350	Uvdal kraftverk	01.10.1985	50.4	1.36	Relocation 4 km W. Merged series 29310 and 29350.
		01.02.2011	103.9	1.15	Automation.
31410	Rjukan	01.06.2003	28.6	0.92	Relocation 2 km E.
31570	Møsvatn-Haug	01.11.1976	23.2	1.15	Relocation 6 km SE. Merged series 31610 and 31570.
36110	Arendal brannstasjon II	01.06.1973	37.8	0.86	Relocation. Merged series 36100 and 36110.
37230	Tveitsund	01.08.2009	25.8	0.93	Automation.
38600	Mykland	01.01.1991	22.9	0.96	Relocation.
39750	Byglandsfjord-Neset	01.09.2011	58.5	0.84	Relocation 2 km N. Merged series 39710 and 39750.
41090	Mandal III	01.08.2009	30.5	0.72	Relocation 3 km S. Merged series 41110 and 41090.
41550	Ljosland-Monen	01.08.1971	24.5	1.08	Relocation 300 m S. Merged series 41560 and 41550.
41860	Kvineshei-Sørhelle	01.06.1986	28.9	1.15	Relocation 7 km SW. Merged series 41880 and 41860.
42950	Øvre Sirdal	01.01.1975	23.7	1.07	Relocation.
44480	Søyland i Gjesdal	01.01.2008	65.7	1.07	Relocation 300 m NNW.
44520	Helland i Gjesdal	01.05.1998	79.8	1.06	New equipment and new observer. Also possible environmental change.
44900	Oltedal	01.07.1972	26.8	1.11	Relocation 2 km W. Merged series 44890 and 44900.
		01.05.2004	22.8	1.03	Possibly irregular observations.
46150	Sand i Ryfylke II	01.12.1988	33.3	1.07	New building.
46850	Hundseid i Vikedal	01.10.2010	29.6	1.08	Relocation 75 m.
47090	Skjold-Føvik	01.08.1986	39.3	1.07	Relocation 1.5 km E. Merged series 47120 and 47090.
47750	Vintertun	01.07.1973	31.3	1.13	Relocation 5 km SW. Merged series 49250 and 47750.
49080	Øvre Krossdalen	01.07.1966	31.7	1.04	Relocation 4 km E. Merged series 49050 and 49070.
		01.01.2013	30.1	0.88	Relocation 500 m E. Merged series 49070 and 49080.
49800	Fet i Eidfjord	01.10.1974	26.7	0.97	Relocation 3 km W. Merged series 49850 and 49750.
		01.12.2005	39.6	0.82	Automation and relocation 1.6 km S. Merged series 49750 and 49800.
52310	Modalen III	01.11.2008	38.2	0.87	Automation and relocation 2 km NE. Merged series 52290 and 52310.
52750	Frøyset	01.08.2000	58.7	1.15	Environmental change - removed fence and vegetation sometime between 1974 and 2011.
52860	Takle	01.05.2014	22.5	0.87	Automation.
52930	Brekke i Sogn	01.06.1983	68.4	0.95	Environmental change - growing trees south of gauge.
		01.07.1996	27.6	0.87	Relocation.

53101	Vangsnes	01.07.1984	30.9	0.94	Relocation 10 m S. New equipment.
55820	Fjærland-Bremuseet	01.12.2005	47.4	0.91	Automation and relocation 1.4 km S.
56010	Høyanger verk	01.08.1981	45.9	0.91	Relocation 1.5 km W. Merged series 56120 and 56010.
56520	Hovlandsdal	01.10.1977	51.5	0.93	Small relocation.
		01.10.1996	29.7	1.02	Small relocation.
		01.10.2013	35.7	1.11	Relocation 200-300 m SE.
56780	Sygna	01.07.1996	46.1	1.13	Relocation 4 km W. Merged series 56800 and 56780.
57660	Eimhjellen	01.07.1981	52.2	1.09	Relocation 5 km E. Merged series 57640 and 57660.
57810	Svelgen II	01.01.1973	81.4	0.89	Relocation 300 m N. Merged series 57800 and 57810.
59250	Refvik	01.07.1996	43.3	0.72	Relocation 5 km NW. Merged series 59200 and 59250.
60800	Ørskog	01.11.2014	24.6	0.89	Automation.
60890	Brusdalsvatn II	01.01.1973	31.2	0.80	Relocation. Merged series 60900 and 60890.
60945	Ålesund IV	01.07.2009	24.6	0.93	Relocation. Merged series 60970 and 60945.
62900	Eide på Nordmøre	01.07.2001	23.2	0.92	Environmental change - growing vegetation.
63100	Øksendal	01.01.2010	47.8	0.93	Small relocation and new building sometime 2010-2013.
63580	Ångårdsvatnet	01.06.1991	50.3	0.88	Relocation.
65230	Hemne-Lenes	01.04.1998	32.5	0.90	Relocation. Merged series 65220 and 65230.
65270	Søvatnet	01.07.2009	27.5	0.90	Relocation 2 m.
66620	Rennebu-Ramstad	01.08.1992	48.5	0.85	Relocation. Merged series 66600 and 66620.
68270	Løksmyr	01.11.1991	76.3	1.09	Relocation 250 m.
68840	Stugudal-Kåsen	01.07.1978	38.8	1.18	Relocation. Merged series 68800 and 68840.
69100	Værnes	01.09.1996	53	0.92	Relocation 14 m.
69380	Meråker-Vardetun	01.12.1969	26.4	0.93	Relocation. Merged series 69360 and 69340.
		01.09.1994	30.1	0.82	Relocation. Merged series 69330 and 69370.
69550	Østås i Hegra	01.04.1970	51.1	0.85	New observer 1969, 1974 nad 1976. Some vegetation changes 1963-1974, but not close enough to affect gaugecatch.
70850	Snåsa-Kjevlia	01.06.1989	50.2	1.10	Relocation 30 m SW.
71550	Ørland III	01.11.1985	45.5	0.89	Relocation.
71810	Åfjord-Momyr	01.01.1975	27.7	0.99	Relocation. Merged series 71800 and 71810.
		01.09.1988	25.6	1.10	Relocation and new building 1987/88 and dec1991/jan1992.
72650	Overhalla-Unnset	01.06.1977	64.3	0.92	Relocation. Merged series 72700 and 72650.
77850	Susendal	01.07.1988	31.5	1.11	Environmental change - vegetation.
82840	Styrkesnes-Hestvika	01.07.1991	49	0.86	Relocation. Merged series 82860 and 82840.
85540	Leknes i Lofoten	01.06.1977	55.6	1.18	Relocation 150 m SSE.
85660	Reine	01.08.1968	29.6	1.35	Relocation. Merged series 85780 and 85660.
86740	Bø i Vesterålen III	01.07.2003	24.2	0.79	Relocation. Merged series 86760 and 86740.

86950	Alsvåg	01.01.1970	46.7	0.92	Relocation.
89650	Innset i Bardu	01.12.1989	102.9	1.27	Unknown. Possible vegetation changes and irregular observations.
89940	Dividalen	01.12.2009	39.2	1.46	Relocation. Merged series 89950 and 89940.
93301	Suolovuopmi	01.11.2004	33.8	0.85	Automation and relocation. Merged series 93300 and 93301.
93900	Sihccajavre	01.06.2011	53.9	1.39	Relocation 50 m 2009-2012. Somewhat irregular observations. Relocation 2013 and 2016. New building 2013-2016.
95590	Børselv	01.01.1984	34.5	1.15	Relocation. Merged series 95600 and 95610.

6.4 Detected breaks in the Swedish series

Table A4. Date and SNHT-value for the detected breaks in the Swedish series.

Number	Date	SNHT
46081540	1963-07-01	26.1
46081540	2000-03-01	91.6
46081570	1980-07-01	24.9
46092120	1972-06-01	24.5
46092290	2011-02-01	30.1
46092410	1972-03-01	22.5
46092410	2011-04-01	25.6
46112020	1990-05-01	33.9
46114360	1978-06-01	39.2
46132170	1962-10-01	41.6
46132170	2017-06-01	26.2
46132310	1977-02-01	31.3
46133420	1983-06-01	53.4
46144310	1980-05-01	57
46155730	1984-02-01	26.4
46188820	1981-05-01	120.8